

AD-A033 308

GEORGIA INST OF TECH ATLANTA SCHOOL OF AEROSPACE ENG--ETC F/G 21/9.2  
SOLID PROPELLANT ADMITTANCE MEASUREMENTS BY THE DRIVEN TUBE MET--ETC(U)  
AUG 76 B T ZINN, B R DANIEL, W A BELL

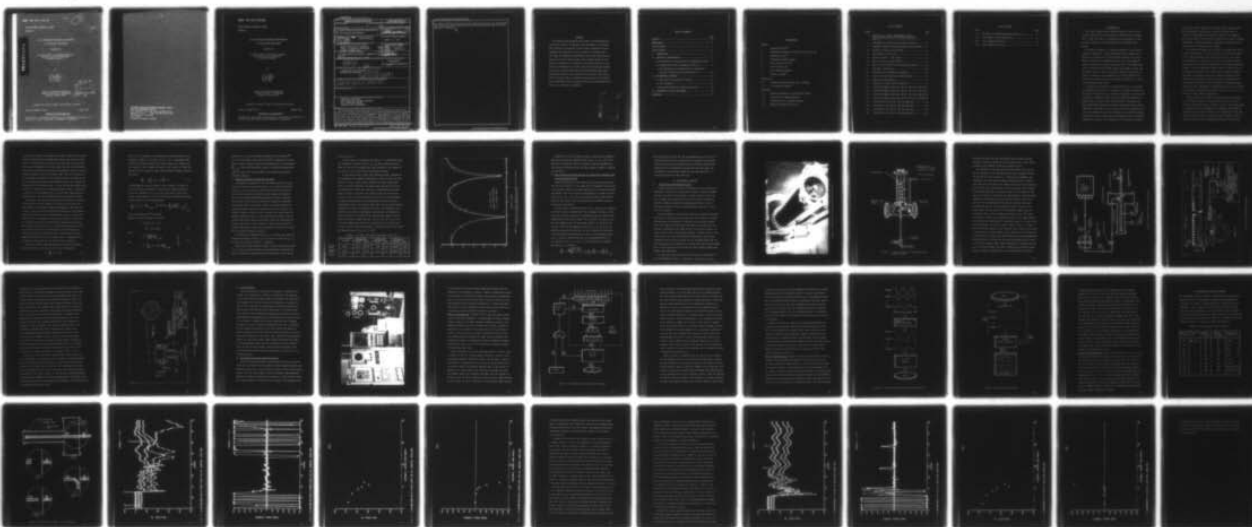
AF-AFOSR-2571-73

AFOSR-TR-76-1211

NL

UNCLASSIFIED

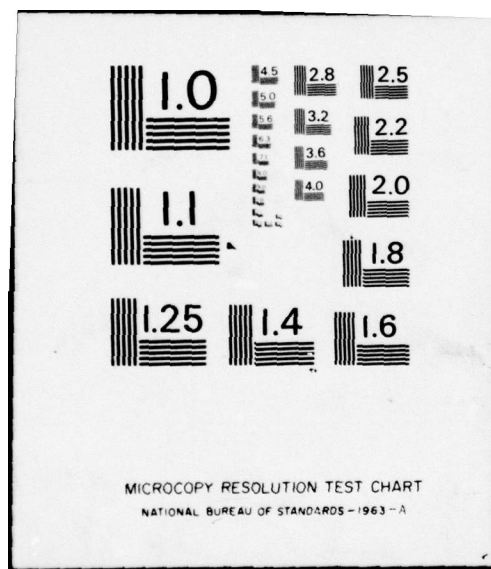
| OF |  
AD  
A033308



END

DATE  
FILMED

2-77



AFOSR - TR - 76 - 1211

AFOSR INTERIM SCIENTIFIC REPORT

AFOSR-TR

ADA033308

SOLID PROPELLANT ADMITTANCE MEASUREMENTS

BY THE DRIVEN TUBE METHOD

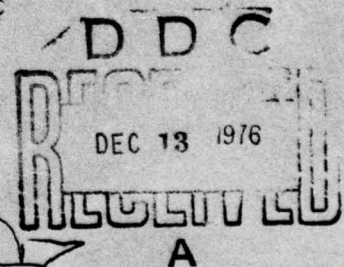
Prepared for

Air Force Office of Scientific Research  
Aerospace Sciences Directorate  
Arlington, Virginia

by

B. T. Zinn  
M. Salikuddin  
B. R. Daniel  
W. A. Bell

School of Aerospace Engineering  
Georgia Institute of Technology  
Atlanta, Georgia 30332



Approved for public release; distribution unlimited

Grant No. AFOSR-73-2571

August 1976

Conditions of Reproduction

Reproduction, translation, publication, use and disposal in whole or in part by or for the United States Government is permitted.

**AIR FORCE OFFICE OF SCIENTIFIC RESEARCH (AFSC)  
NOTICE OF TRANSMITTAL TO DDC**

This technical report has been reviewed and is  
approved for publication release IAW AFR 190-12 (7b).  
Distribution is unlimited.

**A. D. BLOSE**  
Technical Information Officer

**AFOSR - TR - 76 - 121 P**

AFOSR INTERIM SCIENTIFIC REPORT

AFOSR-TR

SOLID PROPELLANT ADMITTANCE MEASUREMENTS

BY THE DRIVEN TUBE METHOD

Prepared for

Air Force Office of Scientific Research  
Aerospace Sciences Directorate  
Arlington, Virginia

by

B. T. Zinn  
M. Salikuddin  
B. R. Daniel  
W. A. Bell

School of Aerospace Engineering  
Georgia Institute of Technology  
Atlanta, Georgia 30332

Approved for public release; distribution unlimited

Grant No. AFOSR-73-2571

August 1976

Conditions of Reproduction

Reproduction, translation, publication, use and disposal in whole or in part by or for the United States Government is permitted.

UNCLASSIFIED

SECURITY CLASSIFICATION OF THIS PAGE (When Data Entered)

REPORT DOCUMENTATION PAGE		READ INSTRUCTIONS BEFORE COMPLETING FORM
1. REPORT NUMBER	2. GOVT ACCESSION NO.	3. RECIPIENT'S CATALOG NUMBER
4. TITLE (and Subtitle) <b>SOLID PROPELLANT ADMITTANCE MEASUREMENTS BY THE DRIVEN TUBE METHOD.</b>		5. TYPE OF REPORT & PERIOD COVERED <b>INTERIM <i>scientific rept.</i> JUN 1975 - JUL 1976</b>
7. AUTHOR(s) <b>B. T. ZINN → M. SALIKUDDIN B. R. DANIEL W. A. BELL</b>		8. CONTRACT OR GRANT NUMBER(s) <b>AFOSR - 73 - 2571</b>
9. PERFORMING ORGANIZATION NAME AND ADDRESS <b>GEORGIA INSTITUTE OF TECHNOLOGY SCHOOL OF AEROSPACE ENGINEERING ATLANTA, GEORGIA 30332</b>		10. PROGRAM ELEMENT, PROJECT, TASK AREA & WORK UNIT NUMBERS <b>681308 9711-01 61102F</b>
11. CONTROLLING OFFICE NAME AND ADDRESS <b>AIR FORCE OFFICE OF SCIENTIFIC RESEARCH/NA BLDG 410 ROLLING ATR FORCE BASE D C 20332</b>		12. REPORT DATE <b>AUGUST 1976</b>
14. MONITORING AGENCY NAME & ADDRESS (if different from Controlling Office) <b>1256p.</b>		15. SECURITY CLASS. (of this report) <b>UNCLASSIFIED</b>
16. DISTRIBUTION STATEMENT (of this Report) <b>APPROVED FOR PUBLIC RELEASE DISTRIBUTION UNLIMITED</b> <b>19 TR-76-1211</b>		15a. DECLASSIFICATION/DOWNGRADING SCHEDULE
17. DISTRIBUTION STATEMENT (of the abstract entered in Block 20, if different from Report) <b>15 ✓ AF-AFOSR-2571-73</b>		
18. SUPPLEMENTARY NOTES		
19. KEY WORDS (Continue on reverse side if necessary and identify by block number) <b>COMBUSTION INSTABILITY SOLID PROPELLANT RESPONSE FUNCTIONS SOLID PROPELLANT ROCKETS IMPEDANCE TUBE MEASUREMENTS</b>		
20. ABSTRACT (Continue on reverse side if necessary and identify by block number) <p>The progress made during the third year of an investigation to measure the response of a burning solid propellant to oscillatory flow conditions is presented. In this study a modification of the impedance tube technique is used to measure the response over a wide range of frequencies. Improvements in the data reduction program are discussed. These include a more accurate method of computing the temperature distribution in the burner tube and a technique for determining the response from pressure amplitude measurements only. A high-pressure facility and minicomputer-based data acquisition system are also discussed in the report.</p>		

DD FORM 1473

EDITION OF 1 NOV 65 IS OBSOLETE

SECURITY CLASSIFICATION OF THIS PAGE (When Data Entered)

AB

SECURITY CLASSIFICATION OF THIS PAGE(When Data Entered)

Data taken at 300 psig indicate that the combustion process of the solid propellant periodically drives and damps acoustic oscillations under most of the test conditions encountered.

SECURITY CLASSIFICATION OF THIS PAGE(When Data Entered)

# ABSTRACT

The progress made during the third year of an investigation to measure the response of a burning solid propellant to oscillatory flow conditions is presented. In this study a modification of the impedance tube technique is used to measure the response over a wide range of frequencies. Improvements in the data reduction program are discussed. These include a more accurate method of computing the temperature distribution in the burner tube and a technique for determining the response from pressure amplitude measurements only. A high-pressure facility and minicomputer-based data acquisition system are also discussed in the report. Data taken at 300 psig indicate that the combustion process of the solid propellant periodically drives and damps acoustic oscillations under most of the test conditions encountered.

ADDITIONAL	
NTIS	Full Text <input checked="" type="checkbox"/>
DTIC	Full Text <input type="checkbox"/>
DAVIDSON	<input type="checkbox"/>
JUSTICE	<input type="checkbox"/>
BY	
DR. [illegible]	
Doc	100-100000
1A	

## TABLE OF CONTENTS

	Page
ABSTRACT . . . . .	ii
NOMENCLATURE . . . . .	iv
LIST OF FIGURES . . . . .	v
LIST OF TABLES . . . . .	vi
I. INTRODUCTION . . . . .	1
II. ANALYTICAL INVESTIGATIONS . . . . .	4
A. Determination of the Steady State Temperature Profile	4
B. Computational Scheme to Minimize the Error. . . . .	7
C. Error Minimization by Application of a Regression Technique Using Pressure Amplitudes Only. . . . .	10
III. EXPERIMENTAL APPARATUS . . . . .	11
A. High Pressure Experimental Facility . . . . .	11
B. Test Procedures . . . . .	21
C. Minicomputer-Based Data Acquisition System . . . . .	21
IV. EXPERIMENTAL RESULTS AND SUMMARY . . . . .	30
REFERENCES . . . . .	45

## NOMENCLATURE

### Symbols

$i$	imaginary unit, $\sqrt{-1}$
$n$	temperature exponent of viscosity law, see Eq. (2)
$p$	pressure, lbf./ft. <sup>2</sup>
$T$	temperature, degrees Rankine
$u$	axial velocity, ft./sec.
$x$	axial distance, ft.
$\Lambda$	heat transfer parameter
$\rho$	density, slug/ft. <sup>3</sup>

### Superscripts

$(\bar{\phantom{x}})$	variable describing steady state conditions
$(\phantom{x})'$	a perturbation quantity

### Subscripts

$(\phantom{x})_c$	quantity evaluated at the propellant surface
$(\phantom{x})_r$	real part of a complex quantity
$(\phantom{x})_i$	imaginary part of a complex quantity
$(\phantom{x})_w$	quantity evaluated at the wall

# LIST OF FIGURES

Figure		Page
1.	Comparison of an Exact Standing Wave Profile and a Computed Profile with Assumed Experimental Errors. . . . .	9
2.	Photograph of Pressurized Driven Burner Facility . . .	12
3.	Schematic Diagram of Pressurized Driven Burner Facility	13
4.	Schematic of Facility Flow System . . . . .	15
5.	Driven Burner Tube Details . . . . .	16
6.	Propellant Sample Holder Details . . . . .	17
7.	Sample Holder with Ignition Wire . . . . .	18
8.	Sketch of Short Probe Pressure Transducer Adapter . . . .	20
9.	Experiment Control Area . . . . .	22
10.	Data Sampling Instrumentation Schematic . . . . .	24
11.	Signal Processing During Data Sampling Phase . . . . .	27
12.	Data Processing Schematic . . . . .	28
13.	Schematic of Exhaust End Configuration . . . . .	33
14.	E-16-633-563 White Propellant ,742 Hz. 300 psig. Open End	34
15.	E-16-633-563 White Propellant ,742 Hz. 300 psig. Open End	35
16.	E-16-633-563 White Propellant ,742 Hz. 300 psig. Open End	36
17.	E-16-633-563 White Propellant ,742 Hz. 300 psig. Open End	37
18.	E-16-633-564 T-13 ,742 Hz. 300 psig Open End . . . . .	.40
19.	E-16-633-564 T-13 ,742 Hz. 300 psig Open End . . . . .	.41
20.	E-16-633-564 T-13 ,742 Hz. 300 psig Open End . . . . .	.42
21.	E-16-633-564 T-13 ,742 Hz. 300 psig Open End . . . . .	.43

# LIST OF TABLES

Table		Page
I.	The Effect of Assumed Experimental Errors on C. . . . .	8
II.	Tests Conducted with Propellant B . . . . .	30
III.	Tests Conducted with T-13 . . . . .	31
IV.	Tests Conducted with A-15 . . . . .	31

## I. INTRODUCTION

This report summarizes the work done during the third year of research supported by Air Force Grant No. AFOSR-73-2571, initiated July 1, 1973. This grant is concerned with the measurement of the acoustic responses of solid propellants by the impedance tube method.

The acoustic response is an important parameter in the study of combustion instability in solid propellant rockets. Combustion instability is characterized by high amplitude pressure oscillations which are driven by the combustion process. These high amplitude pressure oscillations can cause large variations in the thrust with time; can interfere with delicate control and guidance systems; and, in extreme cases, can lead to structural failures. The acoustic response is a measure of the capability of a specific burning solid propellant to initiate and sustain combustion instability in a given solid propellant rocket motor.

To analyze the stability of a particular motor, it is necessary to determine the response (or reaction) of the combustion process to the various disturbances (e.g., pressure fluctuations associated with turbulence or combustion noise) inside the combustion chamber. The amplification or decay of these fluctuations will depend upon the phase relationship between the pressure oscillations and the induced combustion oscillations.<sup>1</sup> If the response time of the combustion process to the combustion pressure oscillation is such that an increase in burn rate occurs during a pressure condensation, then a condition supporting an increase in the amplitude of the pressure oscillation

may result, possibly leading to an unstable engine operation. The question whether instability will occur also depends upon the "losses" in disturbance energy that are present in the combustor. On the other hand, if the burn rate increase occurs during a pressure rarefaction, a condition leading to destructive interference will result and the disturbance will be damped.

The combustion response can be related to the admittance of the burning surface which, in turn, can be used to evaluate the effect of the burning propellant upon the stability of the solid rocket under consideration. Defined as the ratio of the normal velocity perturbation to the pressure perturbation at the burning propellant surface; a positive admittance indicates that the normal velocity and pressure oscillations are in phase and a situation leading to disturbance amplification may result. Negative admittance values indicate that the normal velocity and pressure perturbations are out of phase and damping of the disturbance at the burning propellant occurs. Once determined, the admittance can be used as a boundary condition in combustion instability analysis to predict the stability of a given engine configuration.

The most widely used method for measurement of the admittance is the T-burner. However, several difficulties with this method have been encountered and are discussed in Ref. 2. The present study is concerned with the development of an impedance tube method for measuring the admittances of burning solid propellants.<sup>3</sup> This technique, described in Ref. 2, is known to yield accurate results in studies associated with sound absorbing materials<sup>4</sup> and has been

successfully used in the study of the damping provided by typical solid rocket nozzle configurations.<sup>5</sup>

In this report progress during the past year is discussed and improvements in the supporting theory of the impedance tube technique are presented. These include a more accurate method for determining the steady-state temperature profile in the tube and a method for computing the admittance from pressure amplitude measurements only. In addition, the development of a high pressure facility capable of measuring admittances at pressures up to 500 psig is described. The computerized data acquisition facility which became operational this past year is also discussed and preliminary admittance results at 300 psig are presented.

## II. ANALYTICAL INVESTIGATIONS

The equations describing the behavior of the standing wave pattern inside a driven burner tube are discussed in detail in Ref. 3. Also presented are the techniques used to obtain the admittance of a burning solid propellant from experimentally measured pressure amplitude and phase data taken at discrete points along the standing wave. To further improve the accuracy of the computed admittance values, additional refinements have been incorporated in the data reduction methods during the reporting period, and these are described in this section.

### A. Determination of the Steady State Temperature Profile

In Ref. 3 a method for determining the steady state temperature distribution in the driven burner tube is presented. From this temperature distribution the variation in wavelength along the axis of the tube can be determined and accounted for in the admittance computations. The equation for the temperature distribution is obtained from the steady state energy equation in the tube<sup>3,6</sup> and is given by the expression

$$\bar{T} = T_w + (T_c - T_w) e^{-x/\Lambda} \quad (1)$$

where

$$\Lambda = C \left( 1 + \frac{T_w}{T} \right)^n ; n = 0.68 \quad (2)$$

$T_w$  = temperature at the wall of the tube

$T_c$  = chamber temperature

Since  $T_w$  and  $T_c$  are known from experimental measurement, the constant  $C$  is the only parameter to be resolved in order to determine the temperature distribution in the tube. As shown in Ref. 3, this

constant can be found by measuring the distance between two successive pressure minima along the standing wave pattern. The accuracy of the value of C depends upon how accurately the positions of the pressure minima can be determined. In the past these positions were determined from pressure amplitude data measured by transducers placed at various locations along the walls of the burner tube. Since the locations of the transducers in general did not coincide with the locations of any of the standing wave minima, these minimum positions were obtained by extrapolation of the measured data - a process which inevitably results in errors in locating these standing wave minima. Hence, a search for a method for the determination of the steady state temperature distribution in the tube was undertaken during this reporting period.

An alternate technique which decreases the inaccuracies involved in locating the pressure minima has recently been developed. This method employs the nonlinear regression technique to determine the constant C from the measured amplitude and phase data. The nonlinear regression technique involves determining the value of C which provides the best fit between the theoretically predicted wave pattern in the burner tube and the experimentally measured pressure amplitude and phase data. The best fit is found by determining the value of C which minimizes the root-mean-square deviation between the theoretically predicted burner tube wave structure and the corresponding experimental data. This technique gives a temperature profile which is consistent with the measured wave structure.

To find the minimum root-mean-square deviation, the following function F, which is a measure of the error, is minimized;

$$F = \sum_{i=1}^n (E_i - T_i)^2 \quad (3)$$

In Eq. (3),  $E_i$  represents an experimentally measured quantity (i.e., amplitude or phase) at location  $i$  and  $T_i$  is the corresponding theoretically predicted quantity which depends among other things, upon the constant  $C$ . If a minimum of  $F$  exists with respect to  $C$  then the gradient of  $F$  must vanish at that minimum and the following relationship holds:

$$\frac{dF}{dC} = -2 \sum_{i=1}^n [(E_i - T_i) \frac{dT_i}{dC}] = 0 \quad (4)$$

A Newton-Raphson iterative scheme is used to obtain a solution of Eq. (4) utilizing a linearized version of this equation which involves the expansion of  $T_i$  in a first order Taylor series with respect to the parameter  $C$ .<sup>3</sup> The resulting linear algebraic equation can be expressed in the following form:

$$\sum_{i=1}^n (E_i - T_i^m) \frac{dT_i}{dC} \Big|_{(i,m)} = \left[ (C^{m+1} - C^m) \sum_{i=1}^n \left( \frac{dT_i}{dC} \right)^2 \Big|_{(i,m)} \right] \quad (5)$$

where  $m$  represents the  $m^{\text{th}}$  iteration.

Equation 5 can be rewritten as follows:

$$A^m [C^{m+1} - C^m] = B^m$$

$$C^{m+1} = C^m + B^m/A^m \quad (6)$$

where

$$A^m = \sum_{i=1}^n \left( \frac{dT_i}{dC} \right)^2 \Big|_{(i,m)} \quad \left. \vphantom{\sum_{i=1}^n} \right\} \quad (7)$$

and

$$B^m = \sum_{i=1}^n (E_i - T_i^m) \frac{dT_i}{dC} \Big|_{(i,m)}$$

Equation (7) is a linear algebraic equation for the unknown  $C^{m+1}$  and it can be readily solved once  $A^m$  and  $B^m$  are computed. The computation of these elements requires the determination of the derivative  $\frac{dT}{dc}_{(i,m)}$ . Since these derivatives cannot be determined analytically, numerical values for these derivatives are obtained using finite difference methods.

#### B. Computational Scheme to Minimize the Error:

As discussed in Reference 3, the non-linear regression is used to find the values of the velocity wave  $u'_0$ , pressure wave  $p'_0$  and density  $\rho'_0$  at the propellant surface which give the best fit between the theoretically predicted acoustic pressure distribution and the corresponding experimentally measured acoustic pressures. These values are then used to determine the propellant admittance and response factor. In the last section it has been shown that a similar non-linear regression technique can be used to obtain the constant  $C$  which, in turn, is used to compute the steady state temperature distribution that is consistent with the measured acoustic pressure data. Since these two non-linear regression operations are coupled, they must be solved together to obtain the propellant admittance and response factor data. The manner in which this is being done is briefly explained as follows:

(1) Initially, an arbitrary value of  $C$  is chosen, and, using the "Transmission Matrix" scheme<sup>3</sup>, a set of "initial" values for  $u'_0$ ,  $p'_0$  and  $\rho'_0$  at the propellant surface is computed.

(2) The non-linear regression scheme is used to obtain the values of  $u'_0$ ,  $p'_0$  and  $\rho'_0$  which minimize the root-mean-square deviation between the theoretical equations and the experimental values for the

chosen value of  $C$ .

(3) Once these are determined, the value of  $C$  is recomputed using the determined "optimum" values of  $u'_0$ ,  $p'_0$  and  $\rho'_0$  obtained earlier. Steps (2) and (3) are repeated until the variations in the values of  $u'_0$ ,  $p'_0$ ,  $\rho'_0$ , and  $C$  fall within a specified tolerance.

To check the accuracy of this data reduction scheme, computations were performed for a number of hypothetical cases for which the exact values of  $C$ ,  $u'_0$ ,  $p'_0$  and  $\rho'_0$  were assumed to be known. Using these values as initial conditions, the burner tube equations were solved to determine the "exact" wave structure in the hypothetical burner tube; the latter is plotted (for a specific case) as a solid line in Fig. 1. Next, the points denoted by "x" on Fig. 1 were assumed to be measured pressure data that deviated from the exact data due to experimental errors. This data was then input into the data reduction programs in an effort to determine the error in the admittance computation resulting from experimental inaccuracies. An arbitrary initial value for  $C$  was chosen and the computational scheme discussed earlier was used to compute the wave structure and the desired value of  $C$ . The computed wave structure is represented by the dashed line in Fig. 1 and the table below provides a comparison between the "exact" and computed values of  $p'_0$ ,  $u'_0$ ,  $\rho'_0$  and  $C$ .

TABLE I. The Effect of Assumed Experimental Errors on  $C$

	Heat Transfer Parameter $C$	Pressure $p'_0$		Velocity $u'_0$		Density $\rho'_0$	
		Amplitude in db	Phase in Deg.	Amplitude Ft/Sec	Phase in Deg.	Amplitude Slug/ft <sup>3</sup>	Phase in Deg.
Correct Values	0.943	145.4	230.2	1.48	-21.4	$.612 \times 10^{-6}$	229.0
Computed Values	0.972	145.8	229.9	1.30	-18.2	$.647 \times 10^{-6}$	228.7
Guessed	2.0						

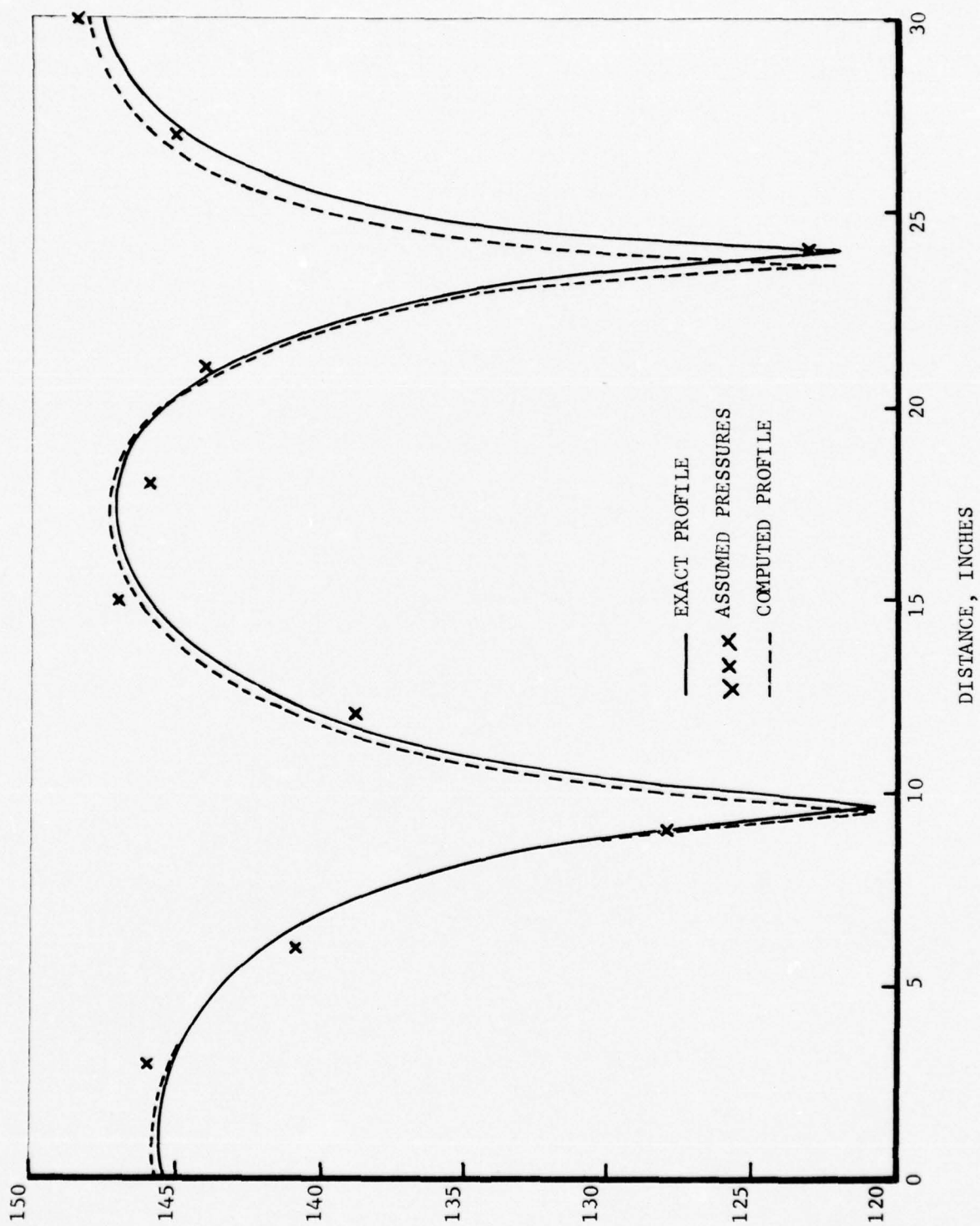


Figure 1. Comparison of an Exact Standing Wave Profile and a Computed Profile with Assumed Experimental Errors.

Examination of the data shown in Table I indicates good agreement between the assumed and computed values of  $u'_0$ ,  $p'_0$ ,  $\rho'_0$  and C even when small experimental errors are present. This good agreement provides further confirmation that the data reduction program is working satisfactorily.

### C. Error Minimization by Application of a Regression Technique Using Pressure Amplitudes Only

Before incorporation of the computerized data acquisition system into the test procedure, it was found that the magnitude of the errors in the measured phases at low amplitudes near the pressure minima were unacceptable. This necessitated the development of a scheme to obtain values of  $u'_0$ ,  $p'_0$  and  $\rho'_0$  at the propellant surface using pressure amplitude data, which could be measured within acceptable tolerance near the pressure minima.

In this scheme, the starting values of  $u'_0$ ,  $p'_0$  and  $\rho'_0$  are computed as before<sup>3</sup> using the transmission matrix technique. However, in this case, the non-linear regression is performed using only pressure amplitude data. In the earlier scheme<sup>3</sup> the derivatives of both the real part and imaginary parts of the complex pressure are obtained with respect to the real and imaginary values of  $u'_0$ ,  $p'_0$  and  $\rho'_0$ . In the modified scheme these derivatives are used to obtain the derivative of pressure amplitude with respect to the real and imaginary values of  $u'_0$ ,  $p'_0$  and  $\rho'_0$ . Representing the real and imaginary parts of  $u'_0$ ,  $p'_0$  and  $\rho'_0$  by  $z_i$ ,  $i = 1, 2, \dots, 6$  the derivatives of pressure amplitude  $p'_a$  are given by

$$\frac{\partial p'_a}{\partial z_i} = \frac{\partial \sqrt{(p'_R)^2 + (p'_I)^2}}{\partial z_i} = \frac{1}{p'_a} \left( p'_R \frac{\partial p'_R}{\partial z_i} + p'_I \frac{\partial p'_I}{\partial z_i} \right) \quad (8)$$

where  $p'_R$  and  $p'_I$  represent the real and imaginary parts of the oscillatory pressure. Once these derivatives are computed the non-linear regression can be used to minimize the error between theoretically computed and the experimentally measured pressure amplitudes. The development of this modified scheme has been completed and it is currently available for data reduction.

### III. EXPERIMENTAL APPARATUS

#### A. High Pressure Experimental Facility

Previous experiments using the driven burner tube to measure the admittance of burning solid propellants have been limited to chamber pressures less than 50 psig because a suitable acoustic driver capable of higher operating pressures was not available. In addition, pressure transducers capable of withstanding pressures of up to 500 psig and having the desired resolution (i.e. 0.01 psi to 3 psi) were not available.

Recently, however, a high pressure facility designed for operating pressures up to 500 psig has been developed. This facility is capable of determining the admittances of burning solid propellant samples under test conditions simulating actual rocket motor operating conditions. A photograph of the high pressure driven burner facility is shown in Fig. 2 and a corresponding schematic is shown in Fig. 3. The driven burner tube with the propellant sample-holder, the pressure transducer, and the acoustic driver are all contained within the 0 to 500 psig pressurization tank which is equipped with high pressure hinged ports to allow easy access for propellant sample changes, burner tube removal, and maintenance.

Air supply for tank pressurization and the flow requirements of the electropneumatic driver is provided by a 3000 psig, 500 cu.ft.

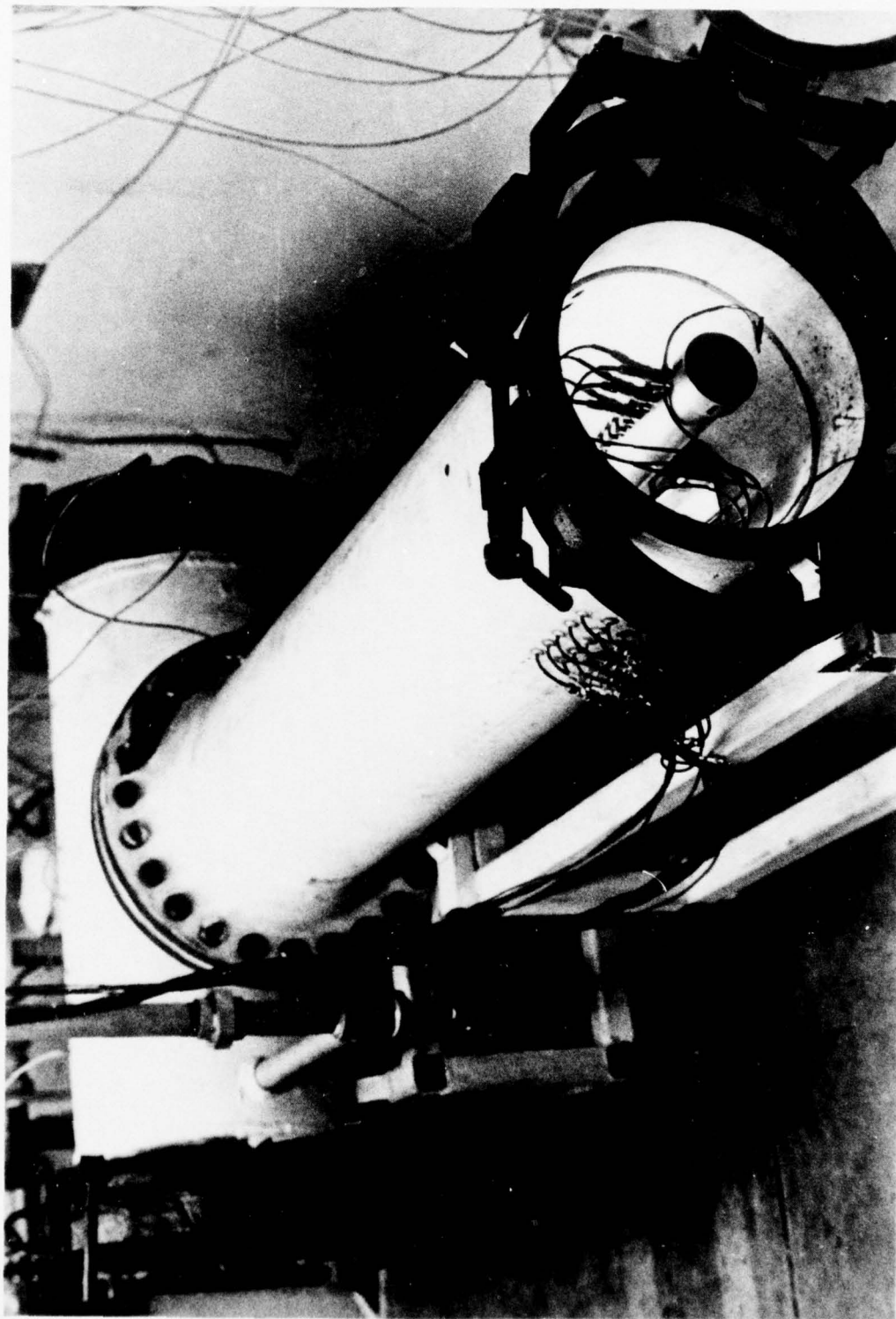


Figure 2. Photograph of Pressurized Driven Burner Facility.

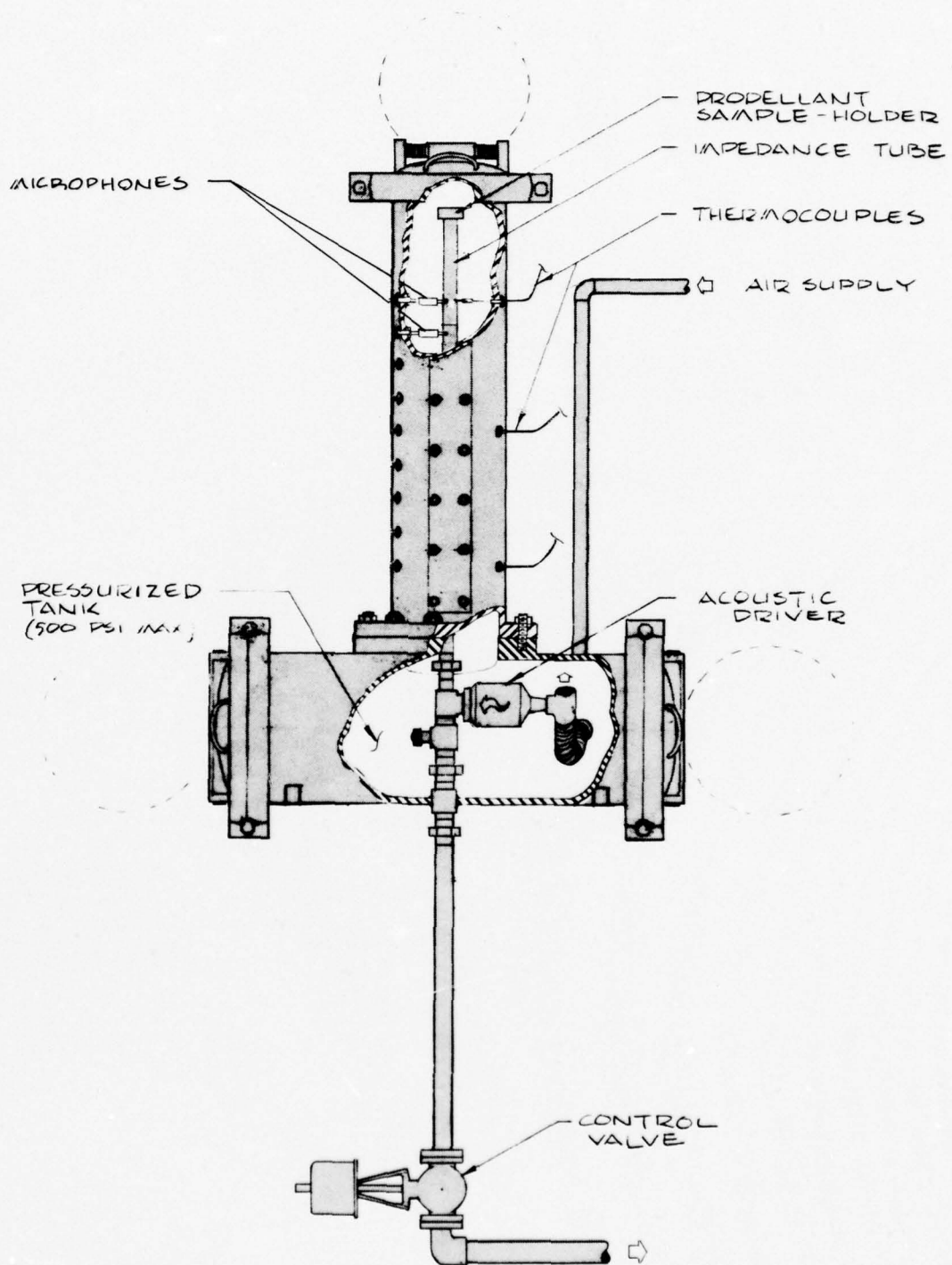


Figure 3. Schematic Diagram of Pressurized Driven Burner Facility.

blow down facility. The tank pressure and driver airflow are maintained by a pressure control valve in the exhaust line of the system as shown in the schematic of the flow system in Fig. 4.

The components of the high pressure driven burner tube facility and the principles of its operation are basically unchanged from the low pressure facility previously in operation. The impedance tube contained in the high pressure tank was fabricated from a stainless steel pipe with a two inch inside diameter. Provisions for a propellant sample holder are included on one end and an acoustic driver capable of developing 4,000 watts of acoustic power is close-coupled to the tube on the other end. Provisions for instrumentation (pressure and/or temperature measurements) have been included along six feet of the tube wall. The instrumentation locations are one-half inch apart measured from the face of the propellant sample. A sketch of the driven burner tube and details of the propellant sample holder are presented in Figs. 5 and 6 respectively. During a test, the propellant sample is ignited by a nichrome wire glued to the sample surface in an "S" shape. A photograph of a propellant sample in a sample holder with the nichrome wire glued in place is shown in Fig. 7. To assure a rapid and uniform ignition of the propellant, the surface of the sample is coated with a thin pyrotechnic mixture comprised of 72.4% potassium perchlorate, 14.8% titanium, 6.9% Boron powder, and 6.0% polyisobutylene binder dissolved in toluene. For ignition the nichrome wire is heated by a 40 volt, 15 ampere power supply. Measuring the standing wave pattern in the driven burner tube with a burning solid propellant sample imposes stringent requirements on the instrumentation. The pressure

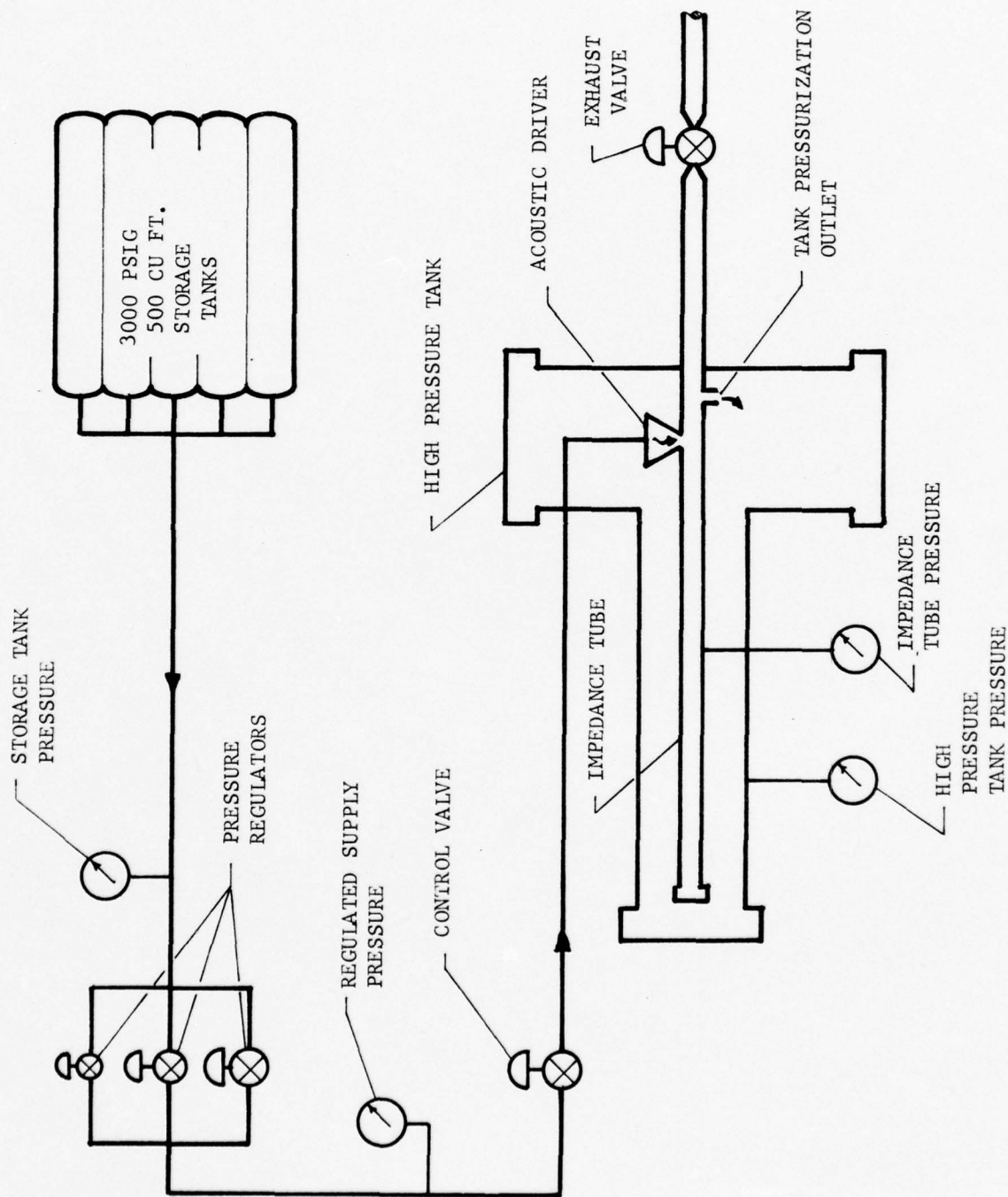


Figure 4. Schematic of Facility Flow System



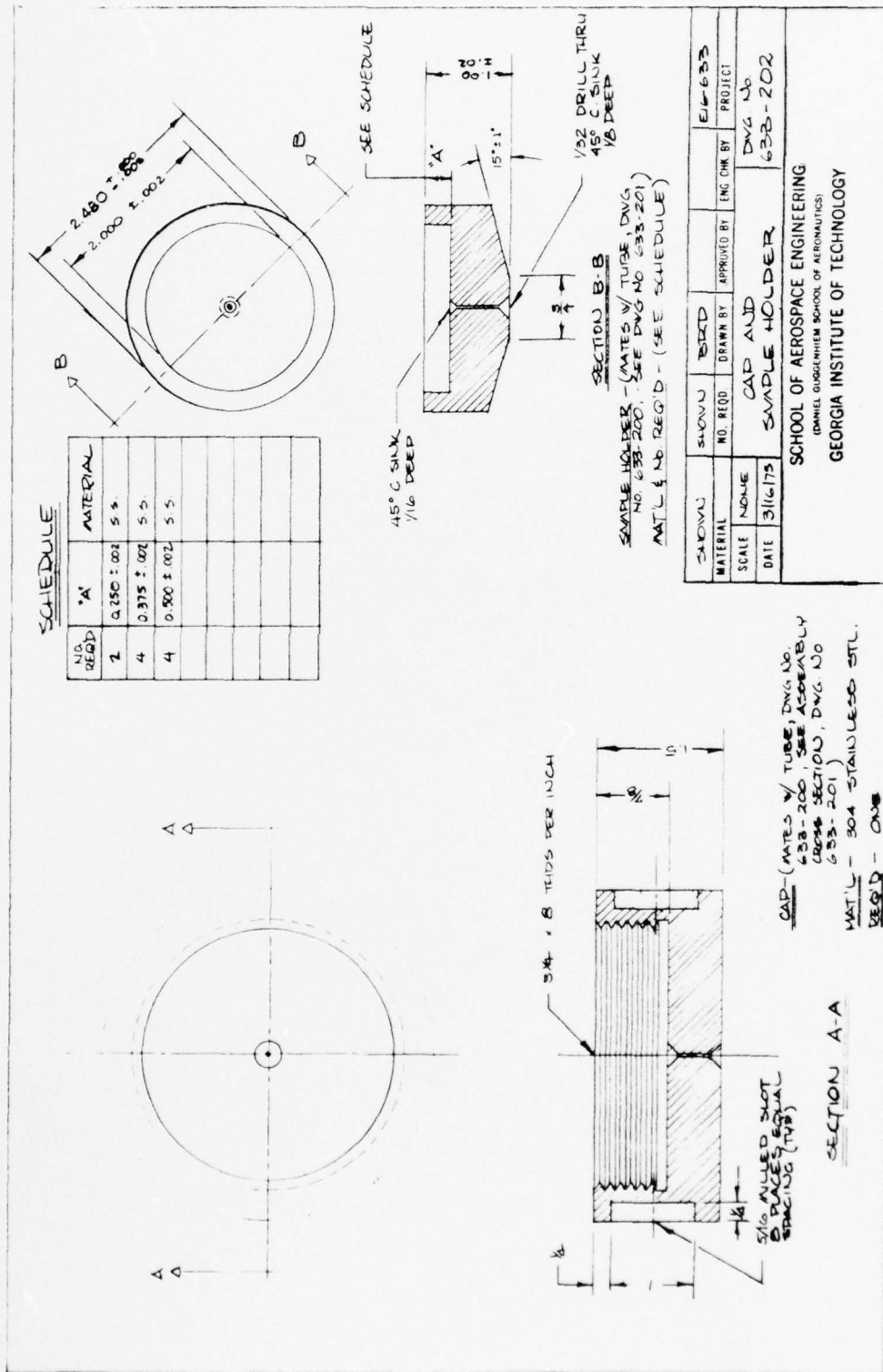


Figure 6. Propellant Sample Holder Details

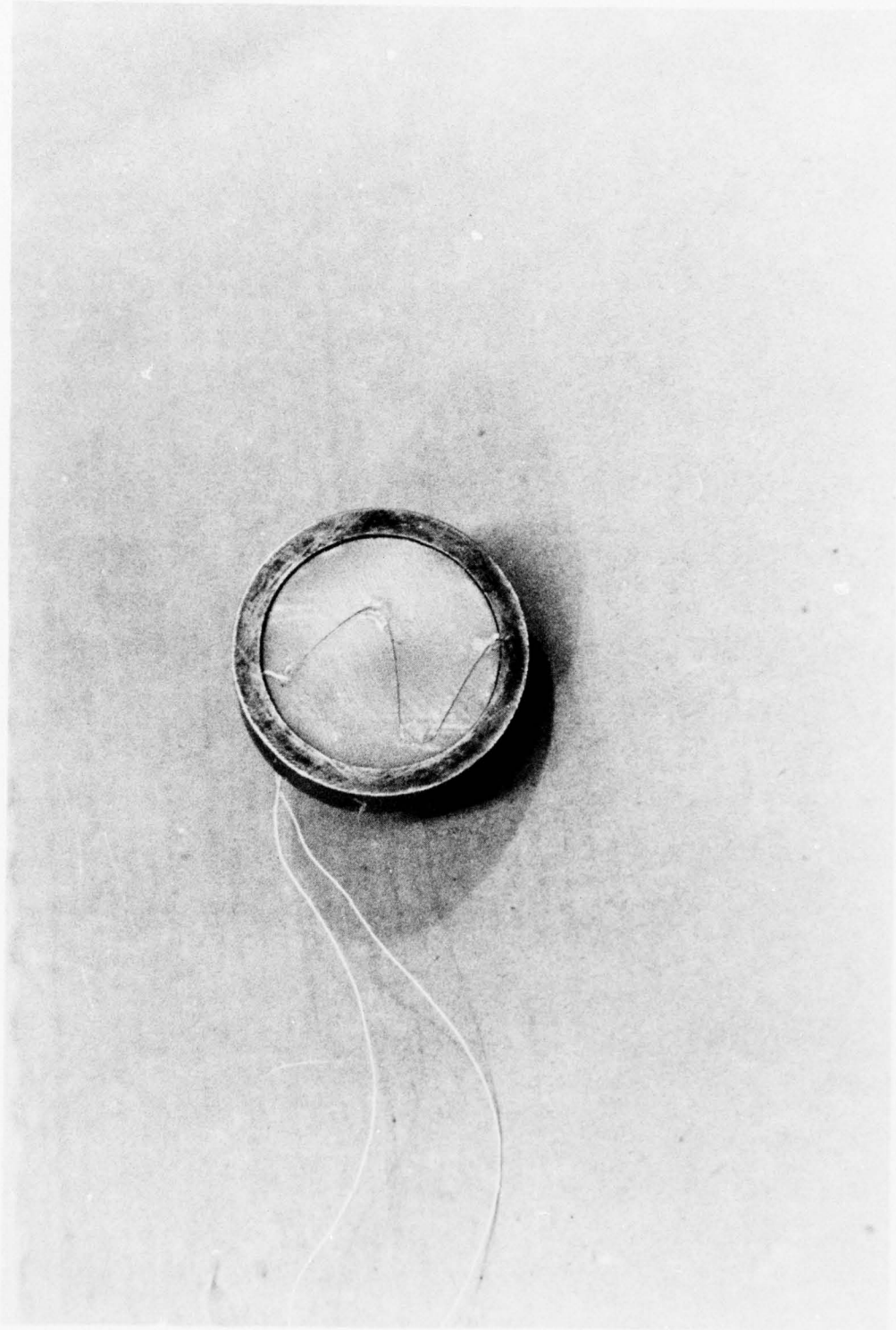


Figure 7. Sample Holder with Ignition Wire.

measurement at high temperatures poses the problem of protecting the highly sensitive transducer diaphragms from the hot gases in the tube. Various methods for the protection of the transducers have been investigated. The semi-infinite tube technique described in Ref. 2 has proven unsatisfactory for high pressure operation because of low frequency resonance in the infinite tube at high pressures. A sketch of an alternate pressure transducer installation utilizing a short adaption is presented in Fig. 8. This adaption has a  $3/16$ -inch inside diameter and it measures  $5/8$ -inch from the transducer face to the inside of the tube wall. Further protection for the transducer is provided by a thin coating of clear silicone grease applied to the transducer diaphragm. Extensive calibration and testing of this short transducer adaptor has been conducted and the results indicate that in the frequency range of interest for this experiment, (i.e., 300 Hz to 1100 Hz), the adapter provides highly satisfactory pressure amplitude and phase measurement characteristics. A detailed discussion with empirical data and design criteria for short probes to be used for dynamic measurements is outlined in Refs. 7 and 8.

The acoustic driver used in the high pressure driven burner tube is a Ling ETP-94 B electropneumatic driver capable of developing 4,000 watts of acoustic power which provides a sound pressure level of 170 decibels in the burner tubes. The driver is close-coupled to the tube wall at the downstream end of the burner tube. The frequency and waveform output of the acoustic driver is controlled by a Spectral Dynamics Oscillator, Model SD104A-5. For this investigation, the waveforms of the pressure oscillations are sinusoidal and the frequency of the oscillations are constant during a given test.

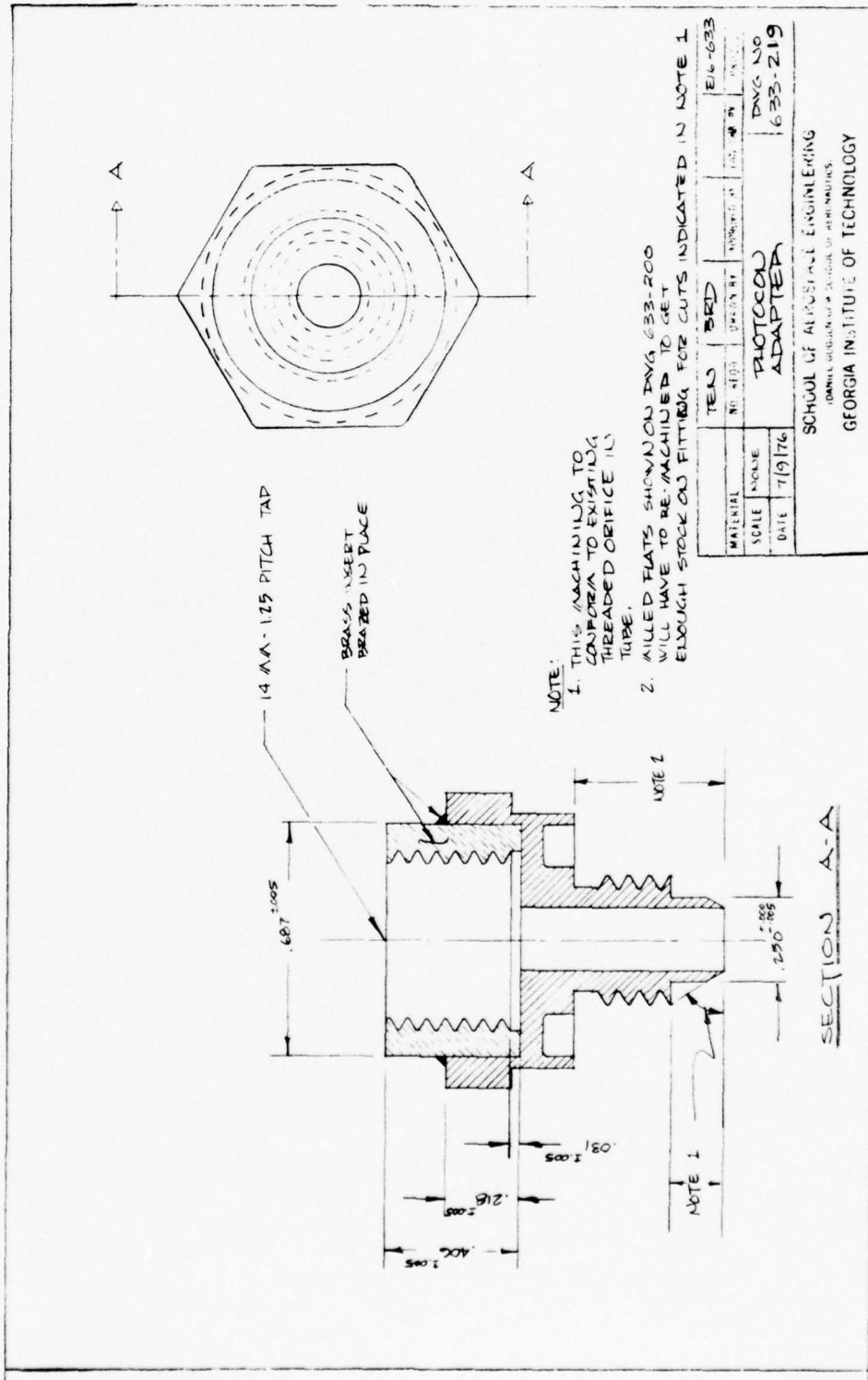


Figure 8. Sketch of Short Probe Pressure Transducer Adapter

## B. Test Procedures.

The data acquisition system and the equipment to establish and monitor test conditions are located in a laboratory area adjacent to the room housing the high pressure driven burner tube experiment. A photograph of the control area for the experiment is presented in Fig. 9. Test conditions are established by slowly pressurizing the high pressure tank housing and the burner tube to the desired operating pressure. The pressurization tank pressure and driver airflow requirements are maintained by the tank pressurization control valve in the exhaust line. With tank pressure stabilized and a standing waveform of a desired frequency established a test run is initiated. The data acquisition period of a test run includes four phases; a brief pre-ignition test period with the acoustic drivers on and test conditions established in the burner tube, ignition of the propellant sample, the propellant "quasi-steady" burning period and the propellant extinguishment phase. The data acquisition period is normally about two and one-half seconds. A more detailed discussion of the data acquisition and data reduction procedures are presented in the following section.

## C. Minicomputer-Based Data Acquisition System

During the reporting period a minicomputer-based data acquisition system was incorporated in the program to obtain improved pressure and temperature data. This system processes the data in three stages. First, during a test the analog signals from the transducer and thermocouple channels are sampled, digitized, and stored at a controlled rate. Next, the stored readings are processed by the computer. The transducer data

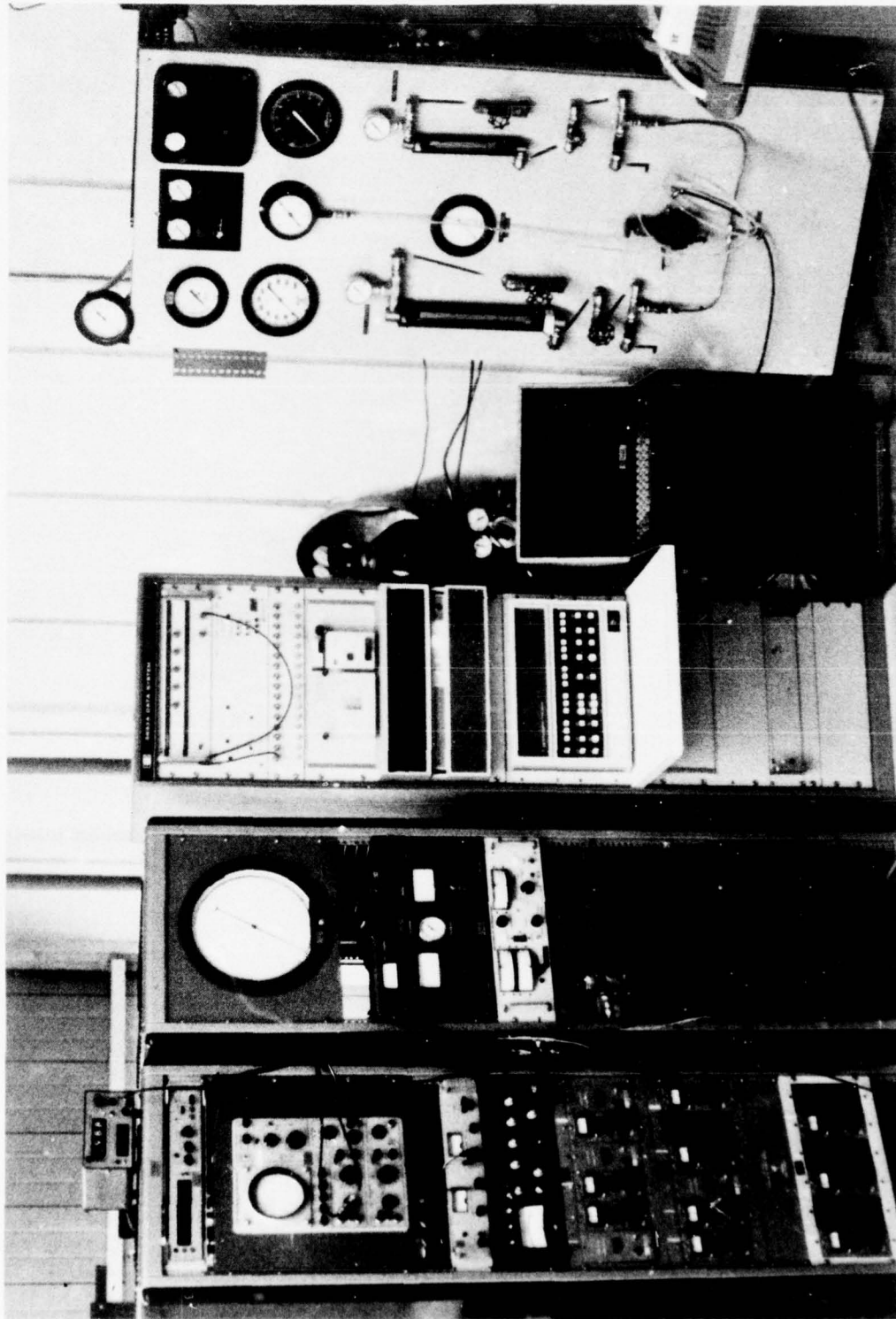


Figure 9. Experiment Control Area.

are digitally filtered and pressure amplitude and phase data are obtained at the frequency of interest. Likewise, thermocouple signals are converted to temperatures. Finally, the pressure and temperature data are printed out and plotted. These values are then used in the data reduction scheme described in Section II to obtain the admittance values. In the remainder of this section, a more detailed description of the data acquisition system is presented.

Phase 1: Data Sampling. As shown in Fig. 10 the data sampling phase involves four major components - a Preston GMAD-11 analog-to-digital converter (ADC), an HP 3220-A frequency synthesizer (pacer), an HP 2100S minicomputer, and a disc storage unit. The ADC is capable of sampling up to 12 channels of input data by use of a multiplexer and has a range of  $\pm 2.56$  volts with a resolution of 20 mv. To obtain maximum signal resolution, the input from the transducer and thermocouple channels are amplified so that the maximum anticipated amplitude for a test is as close to 2.56 volts as possible without exceeding this upper limit.

Upon initiation of a test the following sequence of events occurs as denoted in Fig. 10. (1) The computer initiates a signal to start the analog-to-digital conversion process. (2) The pacer, capable of controlling the sampling rate up to 12 million samples/second, also initiates a signal at the desired sampling rate. In the present experiment up to 12,000 samples per second are taken. When the pacer and computer signals are coincident the sample and hold channels of the ADC go into the "hold" condition so that the input signal voltages at that instant of time are retained. (3) The starting signal from the

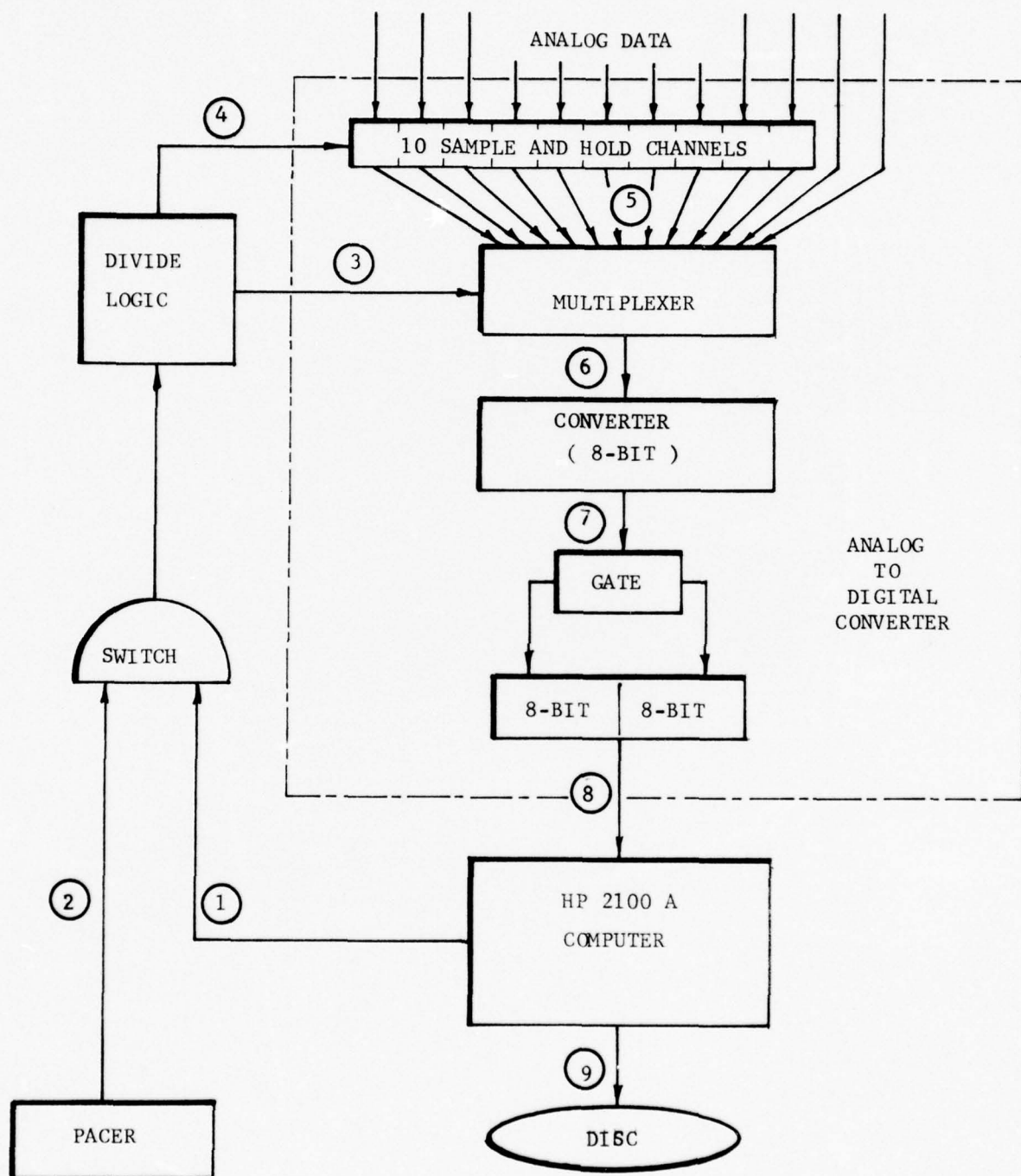


Figure 10. Data Sampling Instrumentation Schematic

switch proceeds to the multiplexer which indexes through the sample-and-hold channels. (4) If the data from all the specified channels have been digitized (determined by the divide logic circuitry), then more data from the input channels are sampled and held. (5) The data from the sample-and-hold device are sequentially transferred two channels at a time by the multiplexer. (6) The voltages from the first of the two channels sampled by the multiplexer enters an 8-bit voltage to binary converter, is digitized, and is stored in a 16-bit output register. (7) The second channel is also digitized and stored in the register. (8) When this process is completed, the computer stores the two 8-bit bytes as a one 16-bit word. By packing the data in this manner the data throughput rate is essentially doubled and increases the upper frequency limit at which reliable data can be acquired. With the present system, reliable pressure data at frequencies of up to 6000 Hz can be obtained. Potentially, the upper frequency limit can be extended to one mega Hz. (9) The packed data word is stored in a buffer in the computer, and the sequence of events is repeated starting with (1).

Before testing, the sampling rate, the size of the data buffer, and the sampling interval are determined. The sampling rate depends upon the frequency of the driven oscillations. The samples are taken rapidly enough to obtain a sufficient number of data points per cycle period for good signal definition. The data buffer and sampling interval are determined by the test conditions. In this study, the ignition and burnout transients produce large variations in pressure amplitude and phase. The sampling interval must be small enough to detect these

variations so that they can be distinguished from the nearly constant amplitudes which occur during the period of quasi-steady burning. On the other hand the sampling interval must be long enough to ensure that the digital filtering interval is sufficient. This last requirement can be relaxed for the tests conducted in the present investigation since the signals thus far encountered have been relatively free of background noise. Once the sampling interval is established the size of the buffer in the computer into which the data is stored is determined.

During a test data are taken at up to 80 sampling intervals of from 10 to 50 milliseconds, and the time between intervals is from 15 to 30 milliseconds. The duration of the run is from two to six seconds for the 3/8" -thick propellant samples used and from 20 to 40 data points are obtained during steady burning. After the digitized data points taken during one sampling interval have been stored, they are then written onto a disc so that room can be made in the buffer to receive the data from the next sampling interval. These steps are depicted in Fig. 11.

Phase 2: Data Processing. During the data processing phase, the disc, computer, and a Tektronix 4012 graphics display terminal are used. The steps involved are shown in Fig. 12. (1) The digitized data taken over one time interval is read from the disc into the computer. (2) The computer software unpacks the data words so that the data from each channel can be processed. From the digitized signals of the transducer channels, the average amplitude and phase over the time interval is obtained. If the time interval is sufficiently short, the time variations

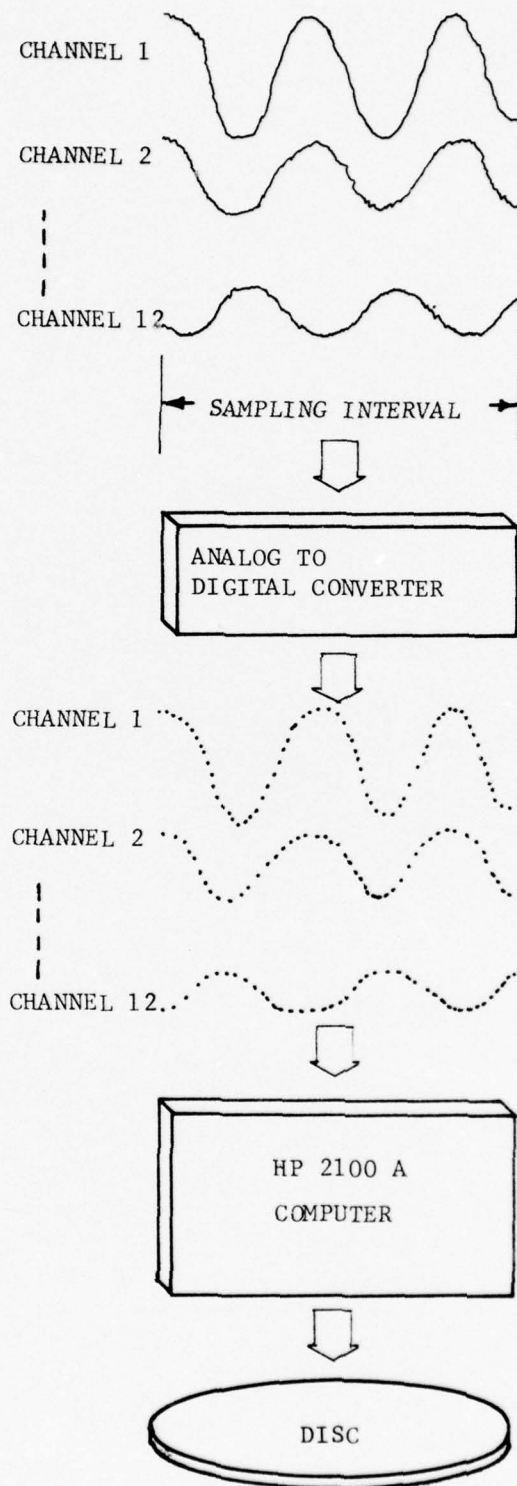


Figure 11. Signal Processing During Data Sampling Phase

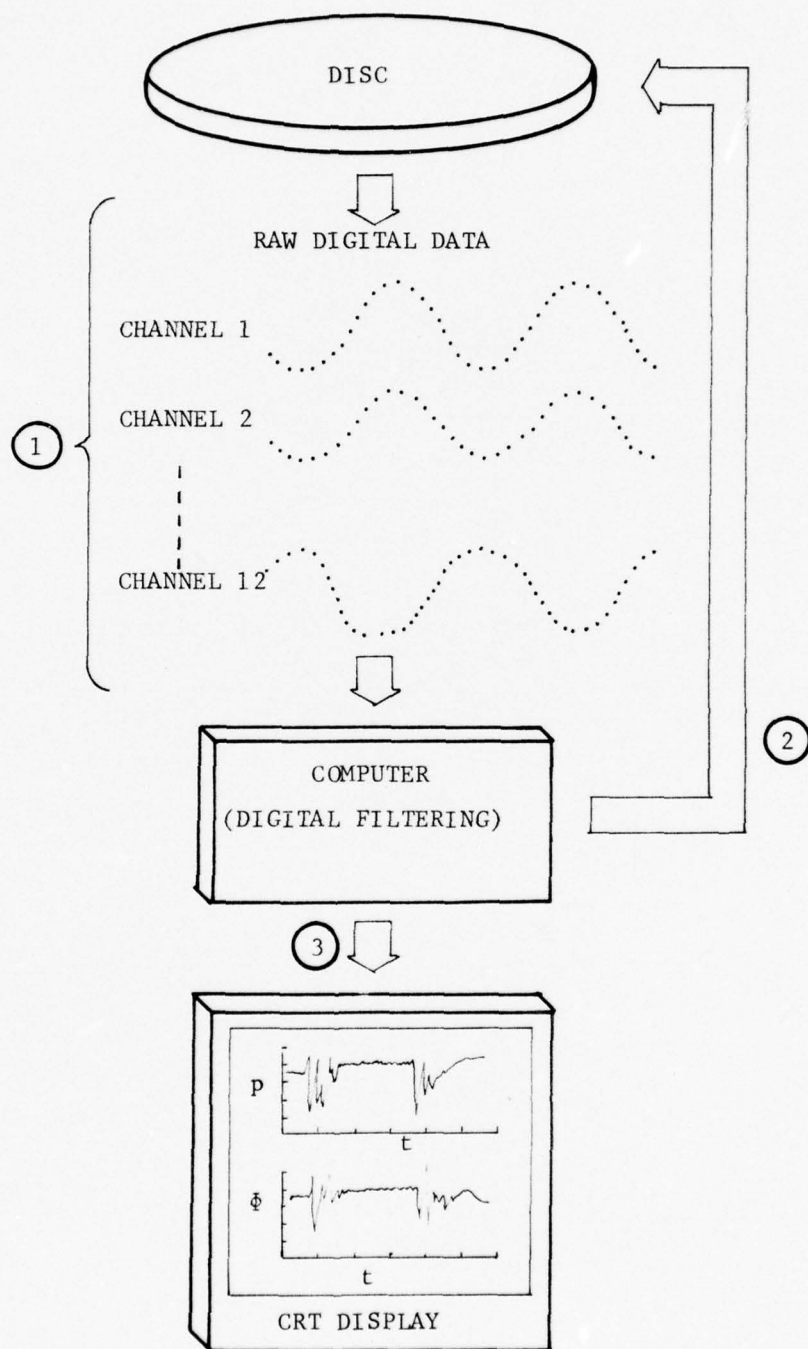


Figure 12. Data Processing Schematic

in amplitude and phase will not be significant and the computed averages will be close to the true value. The average temperature over the time interval is also computed from the digitized thermocouple data by converting the measured voltages to temperature using a Forsyth polynomial expansion obtained from the thermocouple calibration charts. Steps one and two are repeated for each successive time interval. Step (3) consists of taking the resulting amplitude and phase data and plotting them against nondimensional time on the terminal. This provides a check to ensure that proper test conditions were established during the run. The data processing phase generally requires less than five minutes of execution time so that if desired test conditions were not achieved, minimal time is lost between the preliminary data check and retesting. In addition to being displayed on the terminal, the amplitude, phase, and temperature data are also stored on one disc track preassigned to the test which is protected by software. These data can then be displayed at a later date so that minimal time between runs is lost.

Phase 3: Data Presentation. The data presentation phase simply consists of reading the data stored during a run off the disc track assigned to that test and printing or plotting the results. The first step is to plot the amplitude and phase against nondimensional time. From these plots the time intervals at which steady state burning was achieved can be ascertained. At these selected points the amplitude, phase, and temperature data can then be plotted or printed out versus distance. These data are then used in the analyses described in Section II to compute the admittance. This final admittance computation is carried out on a CYBER-70 computer instead of the minicomputer because of the time and storage requirements involved.

#### IV. EXPERIMENTAL RESULTS AND SUMMARY

The experimental efforts during this reporting period were directed toward improving the experimental techniques and determining the admittances of a number of solid propellants at high pressure test conditions. To date, twenty nine tests have been conducted using three different propellants: (1) a T-13 propellant, (2) an undesignated white propellant supplied by Thiokol (referred to as propellant B in this report), and (3) an A-15 propellant. A summary of the tests conducted thus far is presented in Tables II through IV.

TABLE II. Tests Conducted with Propellant B

Expt. No. E-16-633	Propellant Type	Driving Frequency in Hz	Chamber Mean Pressure in psig	Exhaust End Configuration
550	(White), B	625	300	Closed I
559	"	278	300	Open II
561	"	502	300	Open II
563	"	742	300	Open II
565	"	967	300	Open II
573	"	742	300	Closed I
574	"	967	300	Closed I
577	"	742	300	Muffler End IV
578	"	985	300	Muffler End IV

TABLE III. Tests Conducted with T-13

Expt. No. E-16-633	Propellant Type	Driving Frequency in Hz	Chamber Mean Pressure in psig	Exhaust End Configuration	
551	T-13	625	300	Closed	I
560	"	278	300	Open	II
562	"	502	300	Open	II
564	"	742	300	Open	II
566	"	967	300	Open	II

TABLE IV. Tests Conducted with A-15

Expt. No. E-16-633	Propellant Type	Driving Frequency in Hz	Chamber Mean Pressure in psig	Exhaust End Configuration	
552	A-15	625	300	Closed	I
553	"	967	300	Closed	I
554	"	967	300	Closed	I
555	"	1128	300	Closed	I
556	"	967	300	Open	II
557	"		300	Open	II
558	"	1128	300	Open	II
569	"	980	300	Extended Open	III
570	"	912	300	Extended Open	III
575	"	181	300	Closed	I
576	"	181	300	Muffler End	IV
567	"	967	0	Open	II
568	"	181	0	Open	II
571	"	181	0	Closed	II
572	"	967	0	Closed	II

A schematic of the exhaust end configurations used during the tests are presented in Fig. 13. Different configurations were employed to ensure that the conditions at the exhaust end did not affect the relative pressure amplitudes and phases measured along the standing wave, from which the admittance of the propellant is obtained. The data obtained to date indicate that, to within experimental error, no significant change in the admittance values occurs with changing exhaust end conditions.

In Figs. 14 through 17, typical data is presented for a test conducted at 742 Hz with propellant B with an open-ended exhaust condition. Figure 14 is a plot of the pressure amplitude in decibels (re.  $2 \times 10^{-4}$   $\mu$  bar) versus record number for four pressure channels located at different axial stations along the tube. Each record represents a short time interval during which data was recorded by the analog-to-digital converter. Consecutive records correspond to consecutive time instances; hence the abscissa can be considered as representing time.

The data in Fig. 14 can be divided into four phases: (1) the pre-ignition period during which the Ling acoustic drivers are the only source of wave excitation (records 1 to 14); (2) the propellant ignition phase (records 15 to 18); (3) the quasi-steady burning phase during which reliable pressure data can be taken to obtain the burning solid propellant admittance values (records 19 to 40); and the burnout phase (records 41 to 80). During the ignition and burnout phases, the temperature in the tube is changing rapidly with time which produces large variations in the wavelength of the standing wave. Therefore,

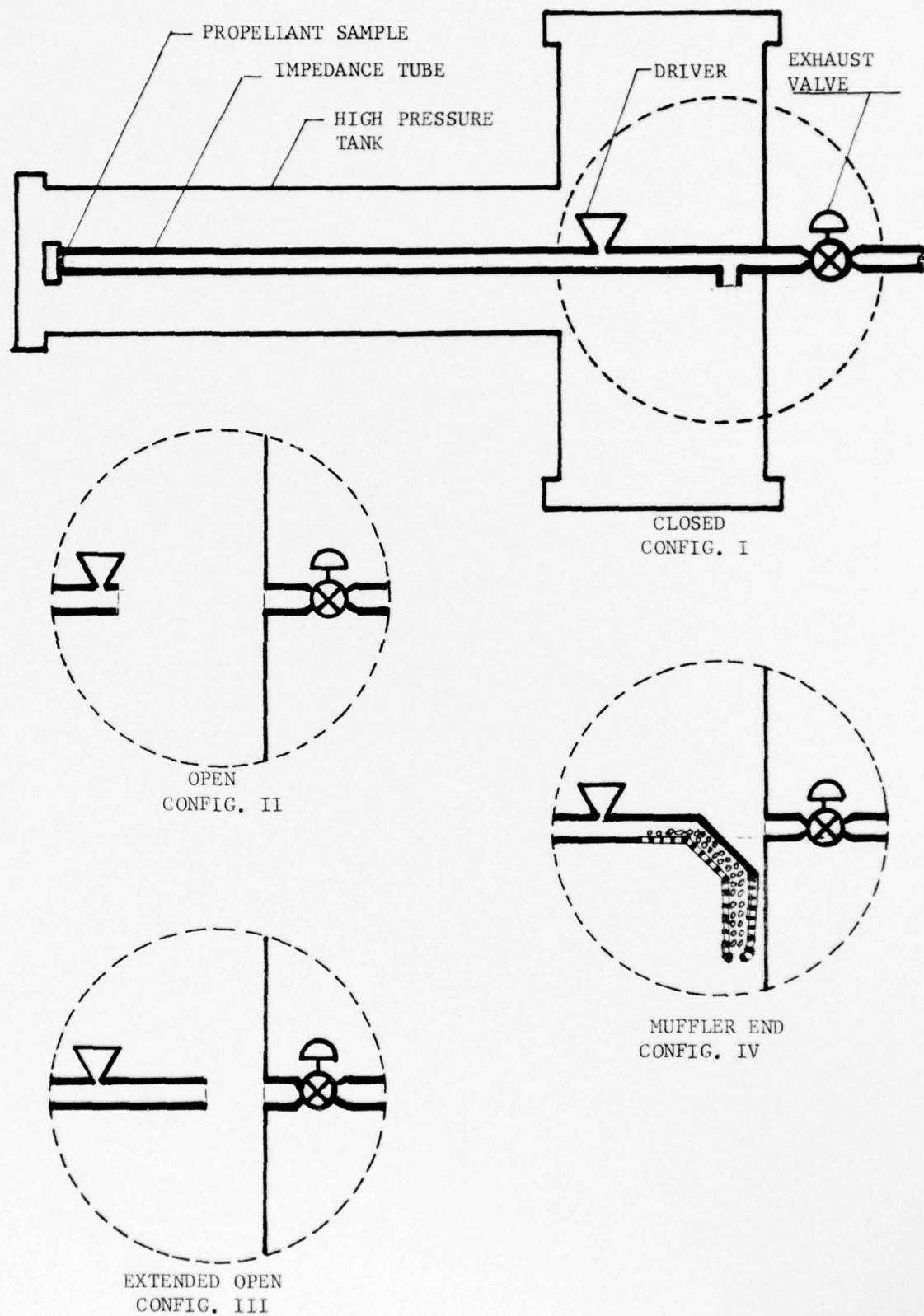


Figure 13. Schematic of Exhaust End Configurations.

CHANNEL = 1 TO 4

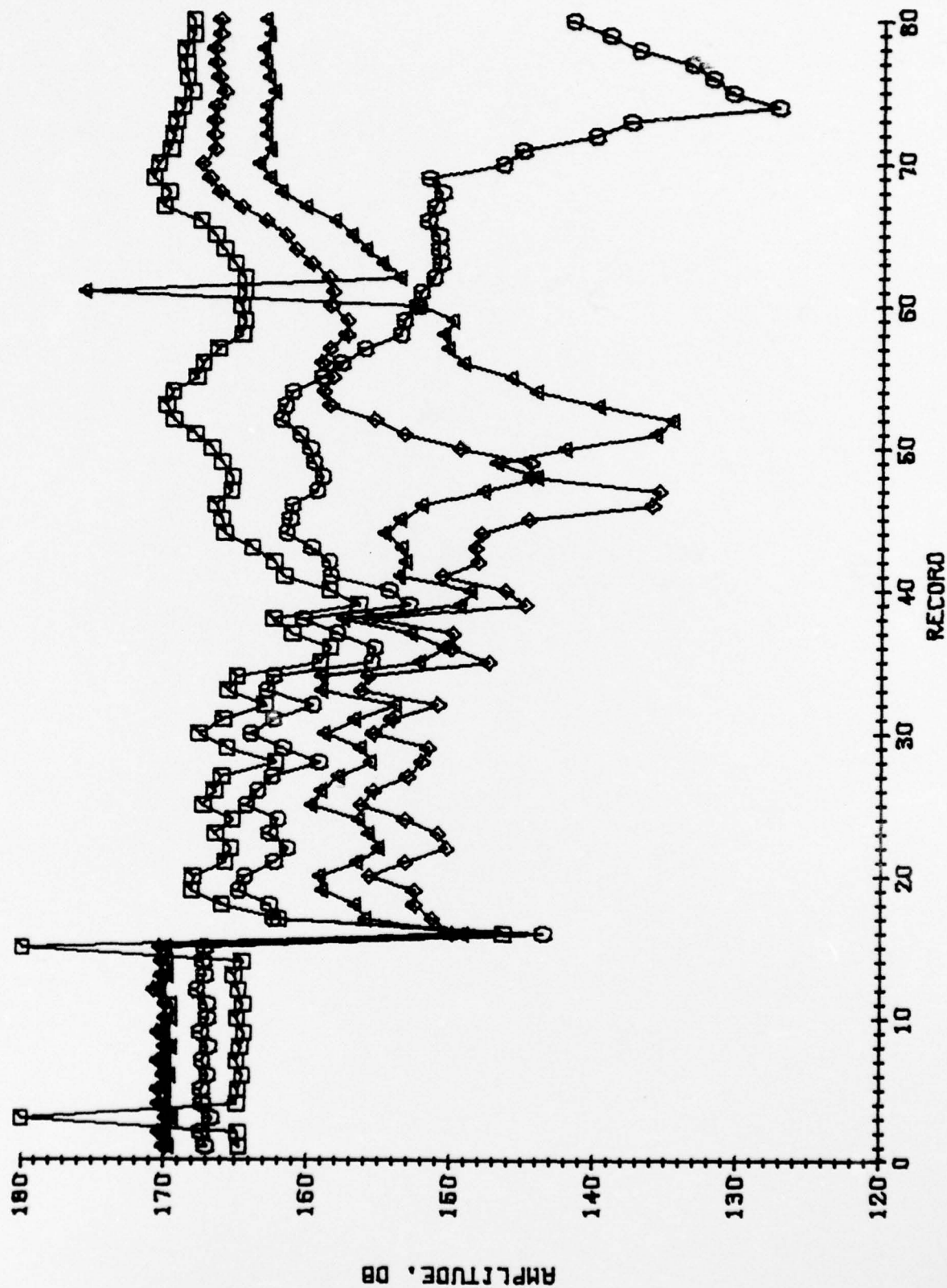


Figure 14. E-18-633-563 WHITE PROPELLANT. 742 HZ. 300PSID. OPEN END.

CHANNEL # 1 TO 4

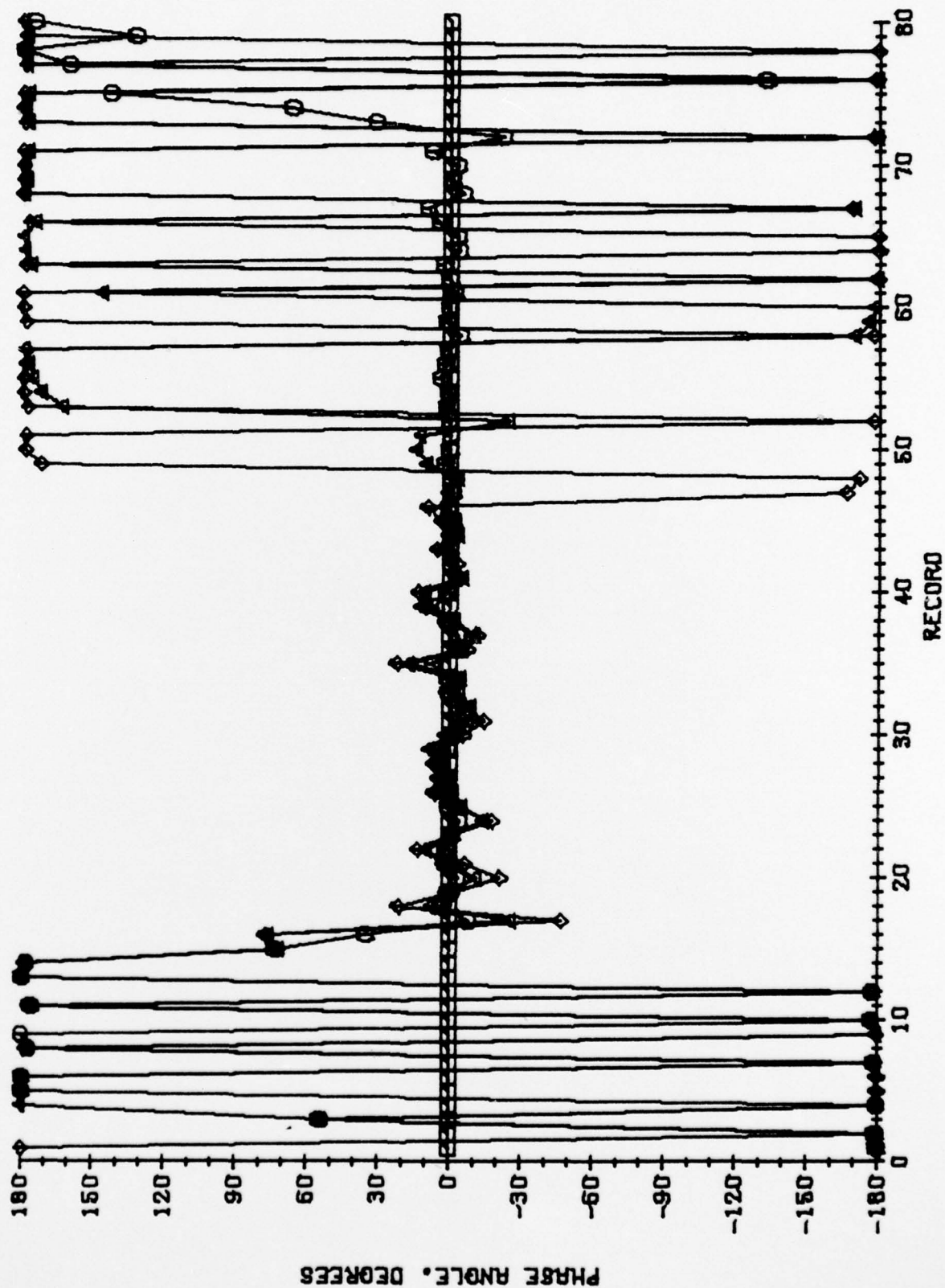


Figure 15.E-10-633-563 WHITE PROPELLANT .742 HZ. 300P910. OPEN END.

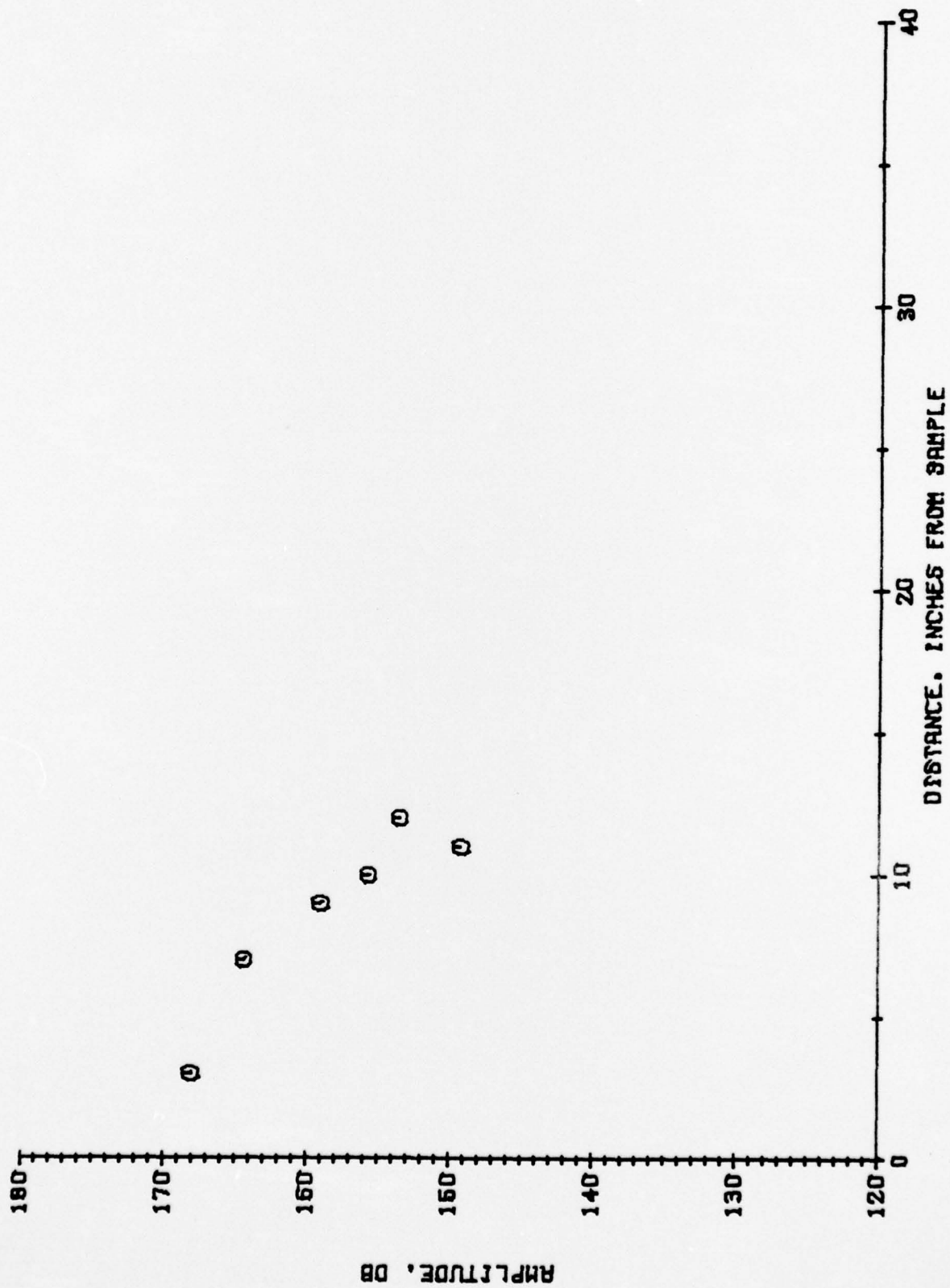


Figure 16. E-10-693-563 WHITE PROPELLANT 742 HZ - 300P910. OPEN END.

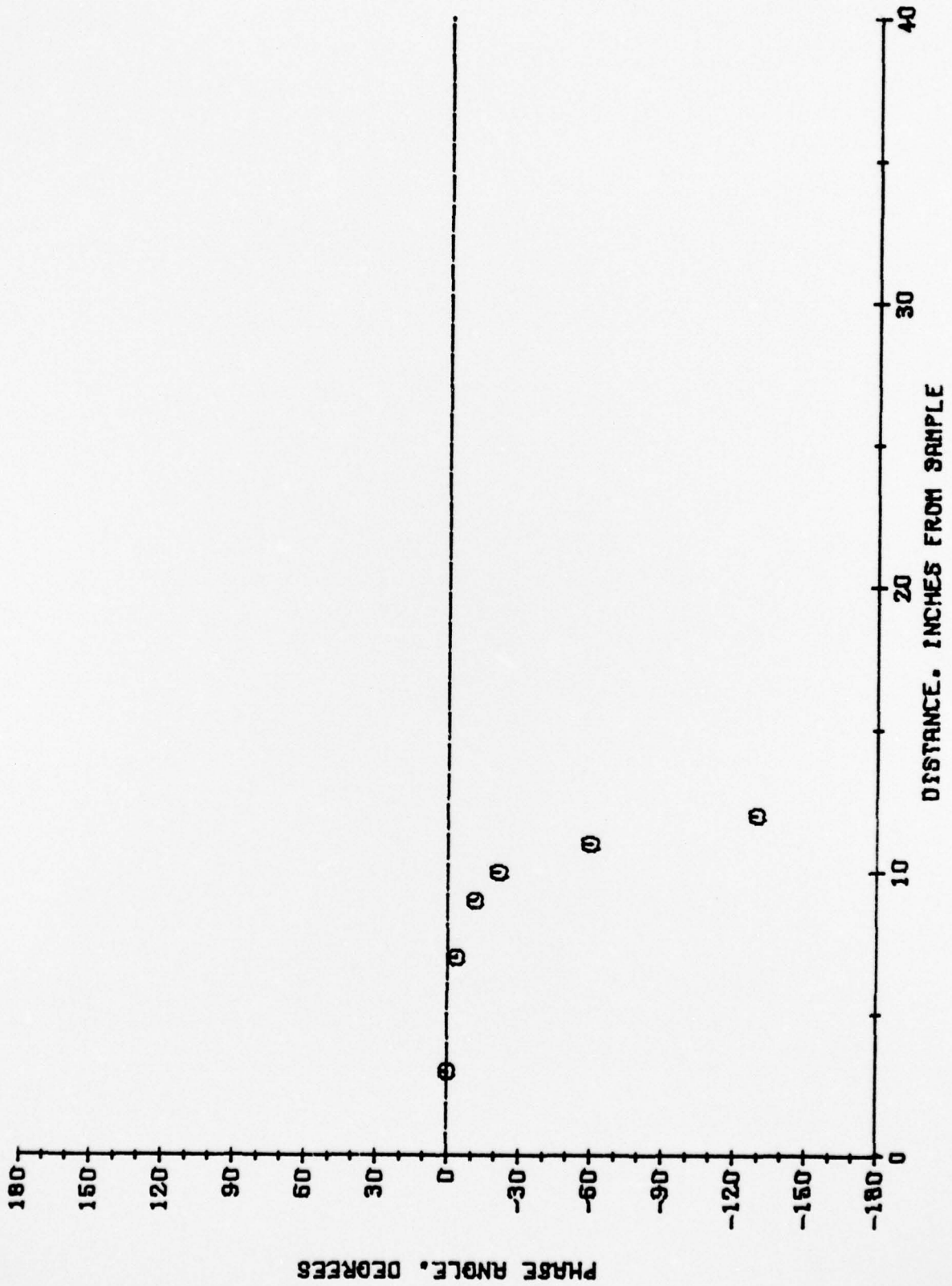


Figure 17. E-10-693-563 WHITE PROPELLANT 742 H3-300P910. OPEN END.

reliable data cannot be obtained during these periods. On the other hand, no significant rapid temperature variations are expected during the quasi-steady phase of the test. Hence, data measured during this period should produce reliable admittance values for the burning solid propellant.

The behavior of the phase with respect to time is shown in Fig. 15. All phases shown in this plot are referenced to the phase measured three inches from the propellant surface. If the phase differences are positive, then the pressure oscillations seven, nine and ten inches from the sample lead the referenced pressure. This type of condition indicates that the incident wave initiated by the acoustic driver is greater in amplitude than the wave reflected from the burning propellant surface; therefore, the combustion process is damping. On the other hand, if the pressure oscillations further from the burning propellant lag the oscillations closest to the sample, then the phase difference is negative and the wave reflected from the propellant is greater in amplitude than the wave incident from the acoustic driver. This condition indicates that the combustion process is driving.

From the phase data in Fig. 15 it appears that the combustion process is randomly damping and driving the acoustic oscillations during the run. This result is unexpected and behavior of this type has not been reported in other studies of burning solid propellants surveyed under this contract. The pressure amplitude and phase variation with distance, taken at record 20, are presented in Figs. 16 and 17. The increasing phase lag with increasing distance from the sample shown in Fig. 17 indicates driving by the combustion process. Based on these

data, an admittance value of 0.1 was computed which means that the combustion process increased the incident wave amplitude by approximately twenty per cent which indicates a strong driving condition at the propellant surface. However, large damping conditions are observed at other times during the burn (e.g. see Record 35). An investigation of the phenomenon is currently underway.

In Figs. 18 through 21 the behavior of the amplitude and phase of the pressure oscillations with respect to time and distance are presented for the T-13 propellant at a frequency of 742 Hz with an open-end exhaust condition. The two "spikes" in the data in Figs. 18 and 21 at records 38 and 58 are erroneous data caused by the ADC digitization process when a significant bit is either erroneously included or excluded. As seen from Fig. 18, the pressure amplitude rises and falls periodically with time during the burn. Since this behavior occurs only after ignition, it is apparently associated with the combustion process. From the phase data presented in Fig. 19, no large driving or damping characteristics are exhibited by the combustion of the T-13 propellant. Instead, it behaves essentially like a hard termination and does not increase or decrease the amplitude of the incident wave significantly. The axial variation of the pressure amplitude and phase at record 45 is shown in Figs. 20 and 21. From the phase plot, Fig. 21, a weak damping by the combustion process is exhibited. However, at other times (i.e. record 50) a weak driving condition is shown.

In almost all tests conducted thus far, at 300 psig, the tested propellants randomly exhibited driving at some times and damping at others. The propellants which are the most unstable (i.e., the A-15 and propellant B) seem to exhibit the largest variation from driving

CHANNEL \* 1 TO \*

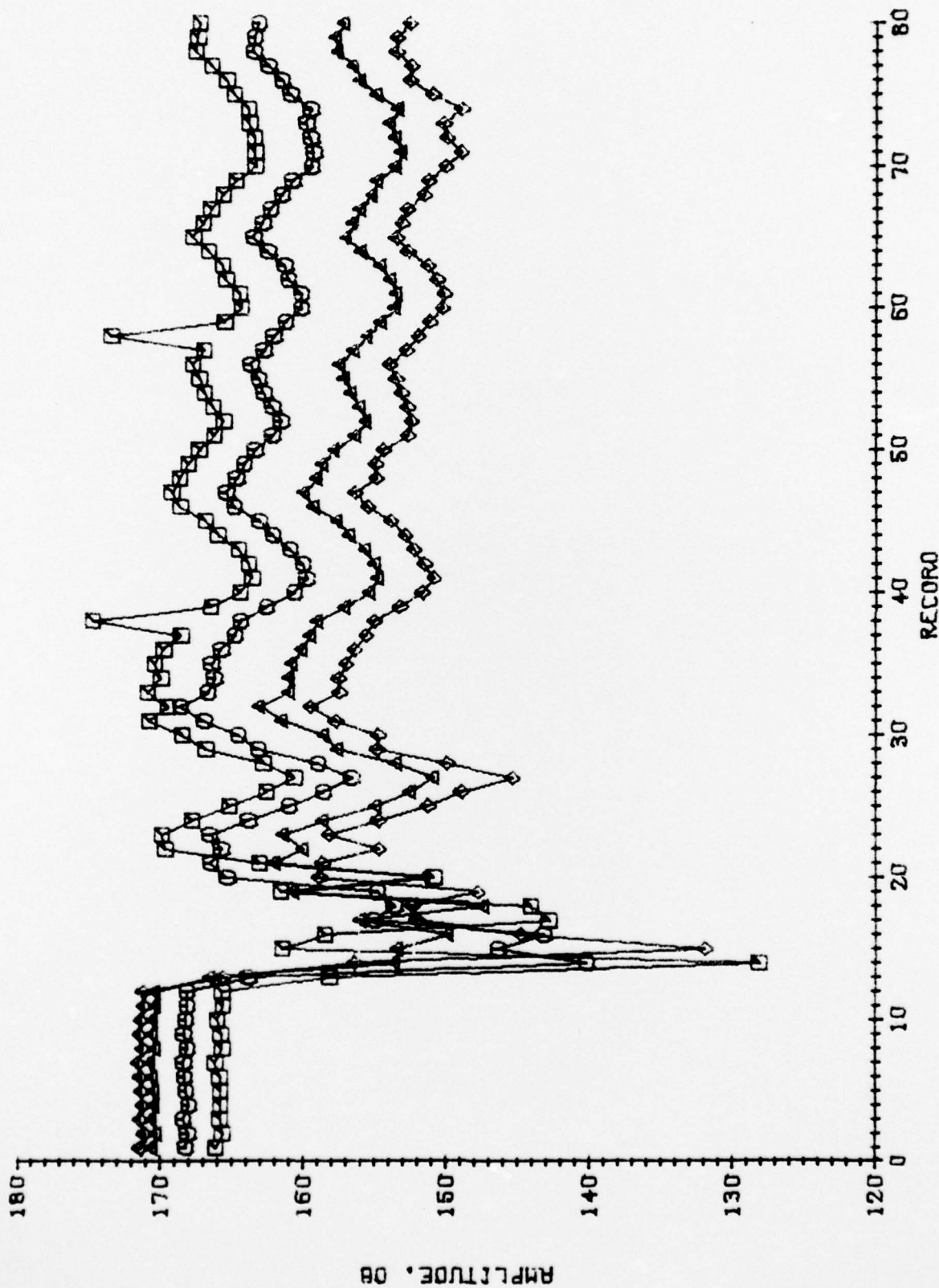


Figure 18. E-16-633-564. T-13.742 Hz..300 PSIG..OPEN END.

CHANNEL \* 1 TO 4

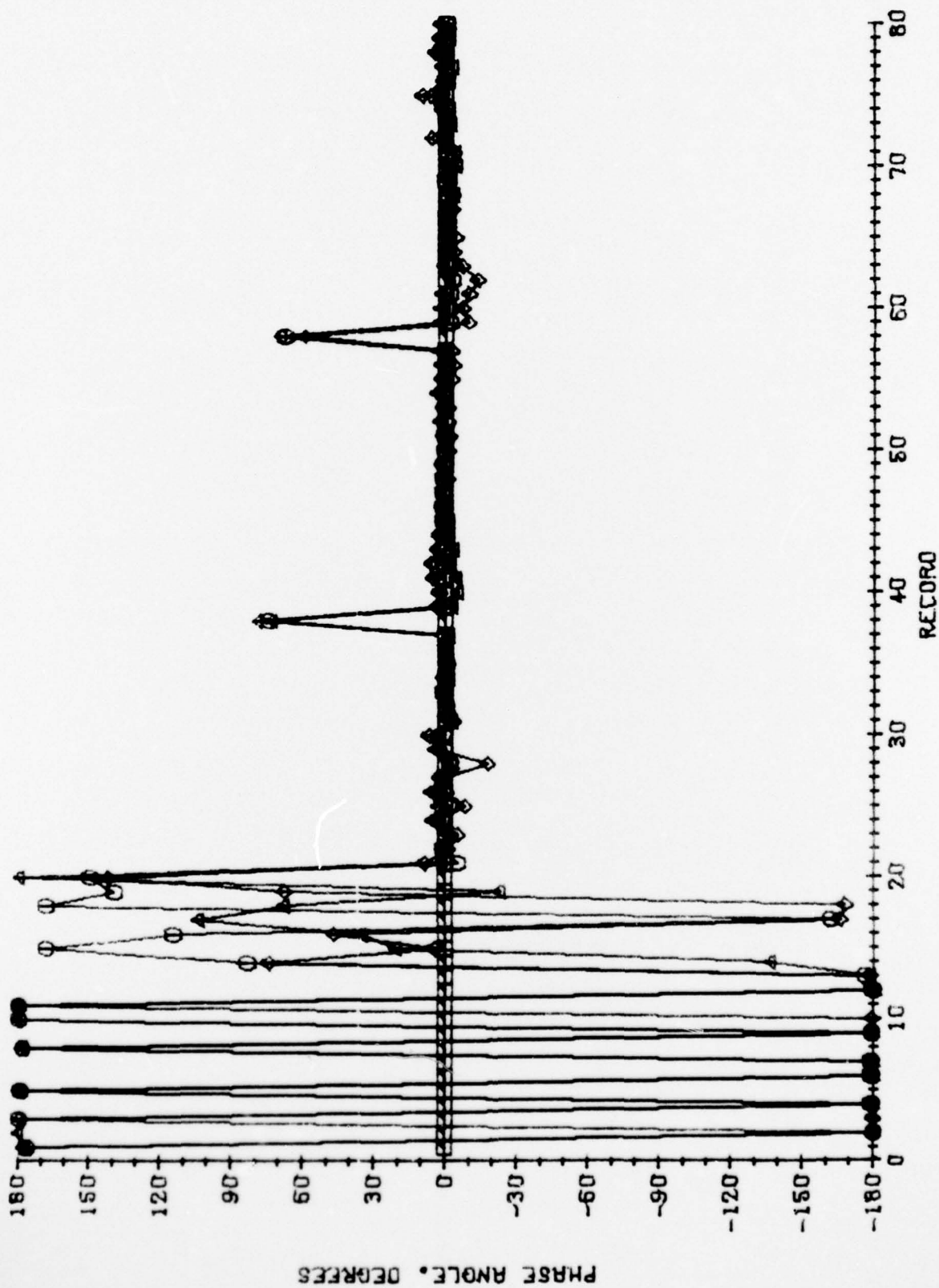


Figure 19. E-16-633-564.T-13.742 HZ--300 PSIG--OPEN END.

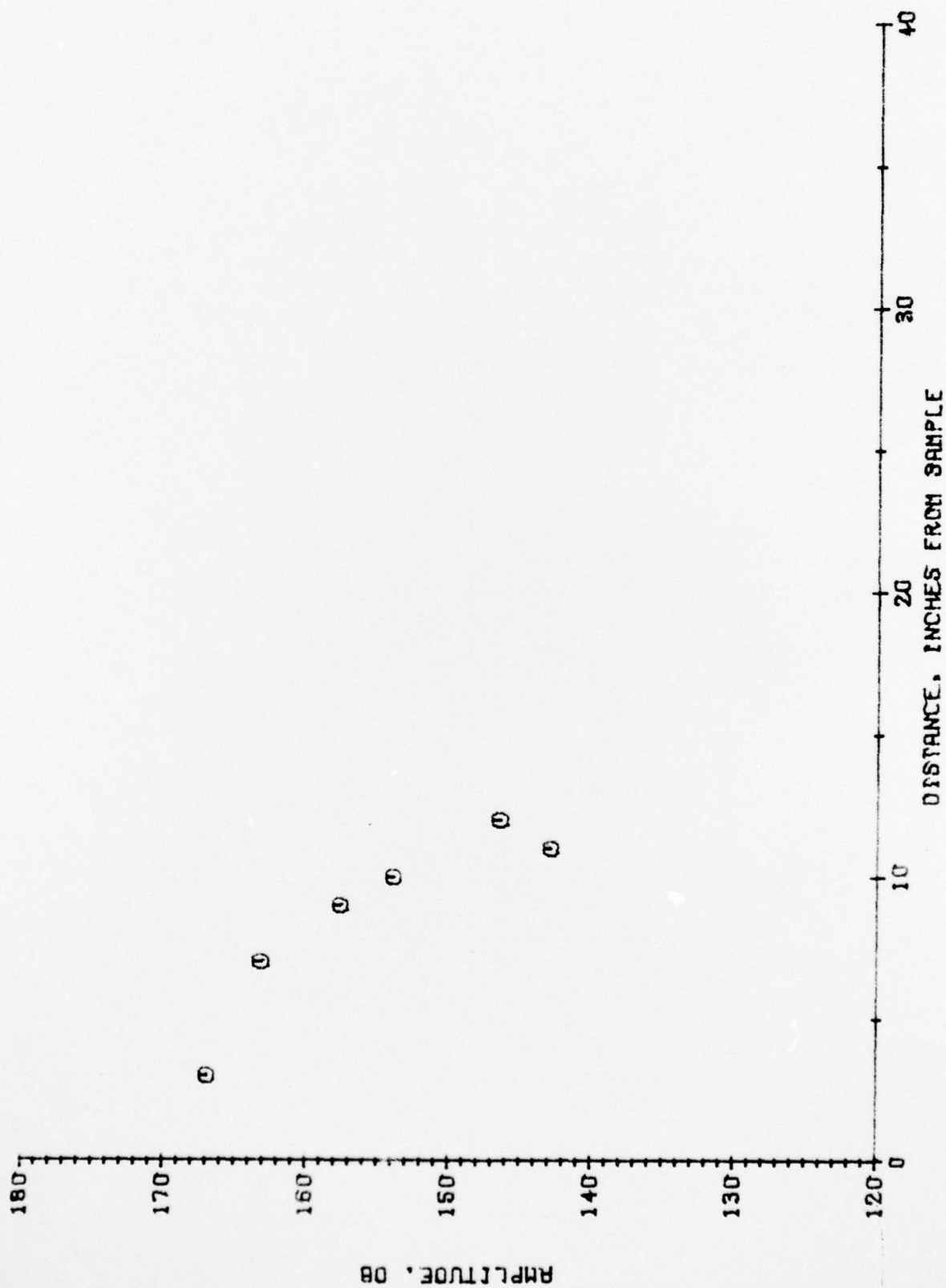


Figure 20. E-16-633-564. T-13.742 Hz. .300 P910-.001 INCH.

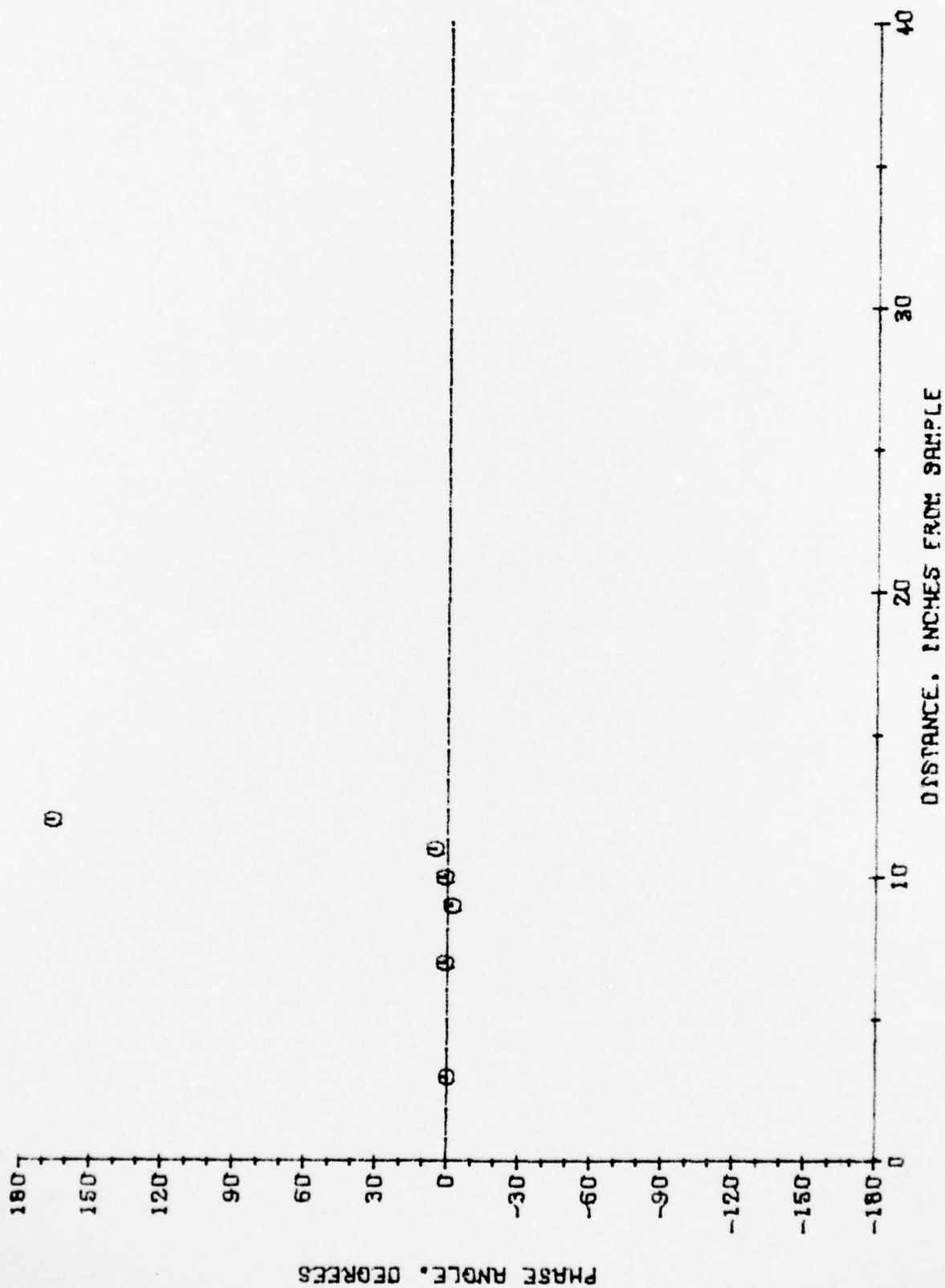


Figure 21. E-10-633-564.  $\Gamma$ -13.742 Hz--300 P510--OPEN END.

to damping whereas the most stable propellant (i.e. the T-13) seems to show the least variation. Current research efforts are concerned with the development of an appropriate explanation for the measured experimental data.

#### REFERENCES

1. Lord Rayleigh, The Theory of Sound, Dover Publications, New York, 1945, Vol. II, Section 322g.
2. Zinn, B. T., Daniel, B. R., Bell, W. A., and Salikuddin, M., "Solid Propellant Admittance Measurements by the Driven Tube Method," Interim Report, AFOSR-73-2571, August 1974.
3. Zinn, B. T., Salikuddin, M., Daniel, B. R., and Bell, W. A., "Solid Propellant Admittance Measurements by the Driven Tube Method," AFOSR-TR-75-1531, August, 1975.
4. Scott, R. A., "An Apparatus for Accurate Measurements of the Acoustic Impedance of Sound Absorbing Materials," Proceedings of the Physical Society, Vol. 58, 1946, pp. 253-264.
5. Zinn, B. T., Daniel, B. R., Janardan, B. A., and Smith, A. J., "Damping of Axial Instabilities by Minuteman II, Stage III, Minuteman III, Stage III Exhaust Nozzles," AFRPL Interim Report, AFRPL-TR-72-71, August 1972.
6. Perry, E. H., "Investigation of the T-Burner and its Role in Combustion Instability Studies," Ph.D. Thesis, Daniel and Florence Guggenheim Jet Propulsion Center, California Institute of Technology, Pasadena, California, May 1970.
7. Nyland, T. W., England, D. R., and Anderson, R. C., "Frequency Response of Short Nozzle Probes," Instruments and Control Systems, August 1973, pp. 27-29.
8. Doebelin, Ernest O. Measurement Systems: Application and Design, McGraw-Hill, Inc., 1966, Section 6.

UNCLASSIFIED

SECURITY CLASSIFICATION OF THIS PAGE (When Data Entered)

REPORT DOCUMENTATION PAGE		READ INSTRUCTIONS BEFORE COMPLETING FORM
1. REPORT NUMBER <b>AFOSR - TR - 76 - 1211</b>	2. GOVT ACCESSION NO.	3. RECIPIENT'S CATALOG NUMBER
4. TITLE (and Subtitle) <b>SOLID PROPELLANT ADMITTANCE MEASUREMENTS BY THE DRIVEN TUBE METHOD</b>	5. TYPE OF REPORT & PERIOD COVERED <b>INTERIM JUNE 1975 -JULY 1976</b>	
	6. PERFORMING ORG. REPORT NUMBER	
7. AUTHOR(s) <b>B.T. ZINN                      M. SALIKUDDIN B. R. DANIEL W. A. BELL</b>	8. CONTRACT OR GRANT NUMBER(s) <b>AFOSR - 73 - 2571</b>	
9. PERFORMING ORGANIZATION NAME AND ADDRESS <b>GEORGIA INSTITUTE OF TECHNOLOGY SCHOOL OF AEROSPACE ENGINEERING ATLANTA, GEORGIA 30332</b>	10. PROGRAM ELEMENT, PROJECT, TASK AREA & WORK UNIT NUMBERS <b>681308 9711-01 61102F</b>	
11. CONTROLLING OFFICE NAME AND ADDRESS <b>AIR FORCE OFFICE OF SCIENTIFIC RESEARCH/NA BLDG 410 BOLLING AIR FORCE BASE, D C 20332</b>	12. REPORT DATE <b>AUGUST 1976</b>	
	13. NUMBER OF PAGES	
14. MONITORING AGENCY NAME & ADDRESS (if different from Controlling Office)	15. SECURITY CLASS. (of this report) <b>UNCLASSIFIED</b>	
	15a. DECLASSIFICATION/DOWNGRADING SCHEDULE	
16. DISTRIBUTION STATEMENT (of this Report) <b>APPROVED FOR PUBLIC RELEASE DISTRIBUTION UNLIMITED</b>		
17. DISTRIBUTION STATEMENT (of the abstract entered in Block 20, if different from Report)		
18. SUPPLEMENTARY NOTES		
19. KEY WORDS (Continue on reverse side if necessary and identify by block number) <b>COMBUSTION INSTABILITY SOLID PROPELLANT RESPONSE FUNCTIONS SOLID PROPELLANT ROCKETS IMPEDANCE TUBE MEASUREMENTS</b>		
20. ABSTRACT (Continue on reverse side if necessary and identify by block number) <b>The progress made during the third year of an investigation to measure the response of a burning solid propellant to oscillatory flow conditions is presented. In this study a modification of the impedance tube technique is used to measure the response over a wide range of frequencies. Improvements in the data reduction program are discussed. These include a more accurate method of computing the temperature distribution in the burner tube and a technique for determining the response from pressure amplitude measurements only. A high-pressure facility and minicomputer-based data acquisition system are also discussed in the report.</b>		

SECURITY CLASSIFICATION OF THIS PAGE(When Data Entered)

✓ Data taken at 300 psig indicate that the combustion process of the solid propellant periodically drives and damps acoustic oscillations under most of the test conditions encountered. ↗

